General Disclaimer

One or more of the Following Statements may affect this Document

- This document has been reproduced from the best copy furnished by the organizational source. It is being released in the interest of making available as much information as possible.

- This document may contain data, which exceeds the sheet parameters. It was furnished in this condition by the organizational source and is the best copy available.

- This document may contain tone-on-tone or color graphs, charts and/or pictures, which have been reproduced in black and white.

- This document is paginated as submitted by the original source.

- Portions of this document are not fully legible due to the historical nature of some of the material. However, it is the best reproduction available from the original submission.

JPL PUBLICATION 78-88

A Review of the State of the Art in Large Spaceborne Antenna Technology

C. A. Smith

November 15, 1978

National Aeronautics and
Space Administration

Jet Propulsion Laboratory
California Institute of Technology
Pasadena, California

HOW TO FILL OUT THE TECHNICAL REPORT STANDARD TITLE PAGE

Make items 1, 4, 5, 9, 12, and 13 agree with the corresponding information on the report cover. Use all capital letters for title (item 4). Leave items 2, 6, and 14 blank. Complete the remaining items as follows:

3. Recipient's Catalog No. Reserved for use by report recipients.

7. Author(s). Include corresponding information from the report cover. In addition, list the affiliation of an author if it differs from that of the performing organization.

8. Performing Organization Report No. Insert if performing organization wishes to assign this number.

10. Work Unit No. Use the agency-wide code (for example, 923-50-10-06-72), which uniquely identifies the work unit under which the work was authorized. Non-NASA performing organizations will leave this blank.

11. Insert the number of the contract or grant under which the report was prepared.

15. Supplementary Notes. Enter information not included elsewhere but useful, such as: Prepared in cooperation with... Translation of (or by)... Presented at conference of... To be published in...

16. Abstract. Include a brief (not to exceed 200 words) factual summary of the most significant information contained in the report. If possible, the abstract of a classified report should be unclassified. If the report contains a significant bibliography or literature survey, mention it here.

17. Key Words. Insert terms or short phrases selected by the author that identify the principal subjects covered in the report, and that are sufficiently specific and precise to be used for cataloging.

18. Distribution Statement. Enter one of the authorized statements used to denote releasability to the public or a limitation on dissemination for reasons other than security of defense information. Authorized statements are "Unclassified–Unlimited," "U. S. Government and Contractors only," "U. S. Government Agencies only," and "NASA and NASA Contractors only."

19. Security Classification (of report). NOTE: Reports carrying a security classification will require additional markings giving security and downgrading information as specified by the Security Requirements Checklist and the DoD Industrial Security Manual (DoD 5220.22-M).

20. Security Classification (of this page). NOTE: Because this page may be used in preparing announcements, bibliographies, and data banks, it should be unclassified if possible. If a classification is required, indicate separately the classification of the title and the abstract by following these items with either "(U)" for unclassified, or "(C)" or "(S)" as applicable for classified items.

21. No. of Pages. Insert the number of pages.

22. Price. Insert the price set by the Clearinghouse for Federal Scientific and Technical Information or the Government Printing Office, if known.

TECHNICAL REPORT STANDARD TITLE PAGE

1. Report No. JPL Pub. 78-88	2. Government Accession No.	3. Recipient's Catalog No.
4. Title and Subtitle A Review of the State of the Art in Large Spaceborne Antenna Technology		5. Report Date November 15, 1978 6. Performing Organization Code
7. Author(s) C. A. Smith		8. Performing Organization Report No.
9. Performing Organization Name and Address JET PROPULSION LABORATORY California Institute of Technology 4800 Oak Grove Drive Pasadena, California 91103		10. Work Unit No. 11. Contract or Grant No. NAS 7-100 13. Type of Report and Period Covered JPL Publication
12. Sponsoring Agency Name and Address NATIONAL AERONAUTICS AND SPACE ADMINISTRATION Washington, D.C. 20546		14. Sponsoring Agency Code

15. Supplementary Notes

16. Abstract

This report studies three classes of antennas (reflectors, lenses, and arrays) with a view toward their use as extremely large space antennas. RF performance characteristics, weight, manufacturing complexity, and cost are discussed for each class. Examples of antennas of each class which have been built or analyzed are described to give an appreciation of current and expected industry capability. Multibeam antennas are discussed. General guidelines are given for use of the appropriate class of antenna to meet certain performance requirements, and recommendations are made for future study. The reflector emerges as the optimum choice for most very large aperture applications, though the lens and array appear ideally suited for use as feeds for multibeam near-field Cassegrain or Gregorian designs.

17. Key Words (Selected by Author(s))	18. Distribution Statement
Spacecraft Communications, Command, and Tracking Components Subsystems	Unclassified - Unlimited

19. Security Classif. (of this report)	20. Security Classif. (of this page)	21. No. of Pages	22. Price
Unclassified	Unclassified	66	

PREFACE

In the spring of 1977, under the auspices of the Director's Office, and organized by Mr. R. V. Powell, a brief but intensive Large Aperture Space Antenna Study was conducted at the Jet Propulsion Laboratory, with participation from several key in-house discipline groups. A question addressed in the study was, "What are the advantages and limitations of large apertures in space?" The study approach included the generation of a number of single point configuration studies addressing feasibility, critical technologies requirements, and expected benefits. This report supports those configuration studies, and may be found useful in other contexts as well.

ACKNOWLEDGMENT

The author acknowledges the support and contributions of the following persons:

R. Munson and G. Sanford of Ball Aerospace Systems Division; C. C. Han, W. Scott, and A. Wickert of Ford Aerospace and Communications Corporation; A. Horvath of General Electric Corporation; C. Strider and D. Nakatani of Hughes Aircraft Company; W. Ackerknecht, D. Bathker, A. G. Brejcha, R. Dickinson, V. Galindo, J. G. Smith and Y. Rahmat-Samii of JPL; P. Byrnes, C. Campbell, W. Chang, and J. Damonte of Lockheed Missiles and Space Company; and J. Crain of Texas Instruments, Inc.

ABSTRACT

This report studies three classes of antennas (reflectors, lenses, and arrays) with a view toward their use as extremely large space antennas. RF performance characteristics, weight, manufacturing complexity, and cost are discussed for each class. Examples of antennas of each class which have been built or analyzed are described to give an appreciation of current and expected industry capability. Multibeam aspects are considered, and general characteristics of multibeam antennas are discussed. General guidelines are given for use of the appropriate class of antenna to meet certain performance requirements, and recommendations are made for future study. The reflector emerges as the optimum choice for most very large aperture applications, though the lens and array appear ideally suited for use as feeds for multibeam near-field Cassegrain or Gregorian designs.

CONTENTS

FIGURES

TABLES

SECTION 1

INTRODUCTION

Due to the recent interest in extremely large space antennas, several general classes of antennas have been promoted as the "best" configuration. In this report three general physical classes (reflectors, lenses, and arrays) will be examined to determine the advantages and limitations of each class with respect to the conflicting requirements (high performance, low weight, and low cost) of space antennas. Data on existing antenna designs will also be presented to define the current industry capability for each antenna class. The data presented here has been gathered from reports in the literature and interviews with individuals in the antenna industry in an attempt to provide inputs to the Large Aperture Space Antenna Study based on practical experience to date. In those cases where no actual measured data was discovered, analytical results were used and identified as such. Using this data the physical classes will be characterized, recommendations will be made concerning future development, and a summary will recommend the most attractive physical configurations for different functional uses.

To minimize confusion, four main functional antenna types will be defined:

(1) A fixed-beam antenna (FBA) is defined as one whose main beam is fixed with respect to the antenna. In addition, the beam usually points in an "easy" or optimum direction, for instance, along the axis of symmetry for a symmetrical paraboloid reflector, or normal to the array for a planar array antenna. Within the spirit of this definition would fall antennas with two or more fixed colocated beams, such as the Voyager spacecraft antenna with fixed-on-axis S- and X-band beams.

(2) A sequential multibeam antenna (SQMBA) is defined as one capable of generating a beam pointing in different directions at different times. The definition implies the ability to scan a fixed-frequency beam with respect to the antenna. An example of this is a phased array antenna with one input and adjustable phase shifters for the array elements. Changing the phase distribution across the aperture by adjusting the phase shifters scans the beam.

(3) A simultaneous multibeam antenna (SIMBA) is defined as one capable of creating noncoherent beams pointing in different directions at the same time. This definition implies the presence of one antenna input port per beam, each input port then corresponding to a certain beam look angle. An example of this is a reflector with two feeds in the focal region. Two

separate beams with different look angles can be created by exciting the inputs to the feeds.

(4) A summed multibeam antenna (SUMBA) is defined as one which creates a broad-shaped beam, perhaps with steerable nulls within it, through the summation of the contributions of many narrow beams, each of which has a different look angle. An example of this is a lens antenna illuminated by several feeds placed in the focal region and connected by a summing network.

SECTION 2

CHARACTERISTICS AND EXAMPLES OF MAJOR ANTENNA CLASSES

In this section physical and RF performance characteristics will be discussed for the three major antenna classes considered. For each class of antenna, examples of actual physical hardware will also be discussed. In many cases it will be noted that the examples do not represent "large" antennas, usually because large physical examples do not exist. However, these examples should help to illustrate the performance achievable by that antenna class.

2.1 REFLECTORS

Reflectors constitute one of the most widely used classes of large antennas. For many years large antennas have been created by using a small feed to illuminate a large reflector. A large body of theoretical and empirical design data exists. A reflector itself is quite broadband, limited at upper frequencies by its roughness. The roughness of the surface causes phase errors in the aperture field of the antenna, resulting in sidelobe level increase and peak gain decrease. Figure 1 shows the gain loss as a function of rms roughness in wavelengths. Figure 2 shows the gain performance versus frequency for a 3-m (10-ft) diameter reflector for three values of surface roughness. The gain increases as the square of the frequency due to the increase in aperture size (measured in wavelengths); however, the exponential increase in gain loss due to surface roughness (also measured in wavelengths) predominates at high frequencies to give an upper limit to efficient reflector performance. Figure 3 (Ref. 18) shows the increase in sidelobe level caused by surface roughness. At frequencies below the roughness limit, the antenna bandwidth is determined by the feed bandwidth.

The doubly curved surfaces used for reflectors tend to partially shadow themselves when sun-illuminated at different angles, creating thermal gradients that cause surface deformations. The resulting phase errors cause gain losses and beam squint. The feeds and feed support structures, mounted in front of the reflector, are also subject to thermally induced deformations that tend to defocus the antenna or cause beam squint.

Reflectors present a design problem that is relatively easy to solve because of the large body of design data available; they are also relatively easy and inexpensive to fabricate and inspect due to the simplicity of the surfaces and the limited number of parts to be inspected.

Reflectors are generally quite lightweight, as can be seen from Table 1, which gives weight and size data for several antennas of each class.

The increased size requirements for spacecraft antennas have surpassed the available launch vehicle shroud or shuttle bay limits. Three methods for creating reflector antennas larger than these limits

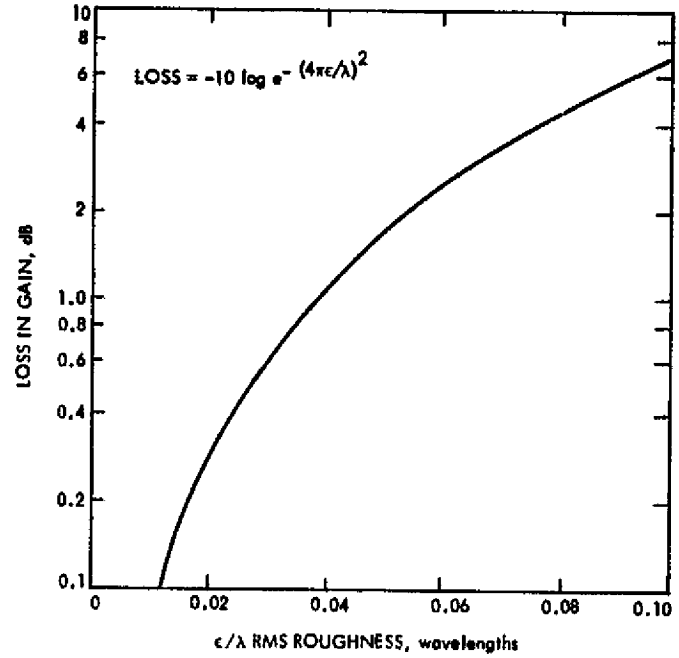

Figure 1. Gain Loss Due to Surface Roughness

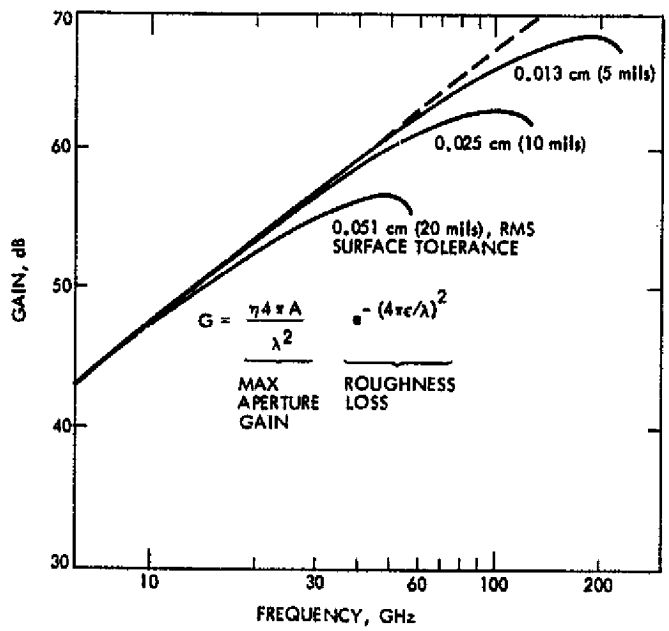

Figure 2. Antenna Gain vs Frequency and Roughness, 3-m Diameter

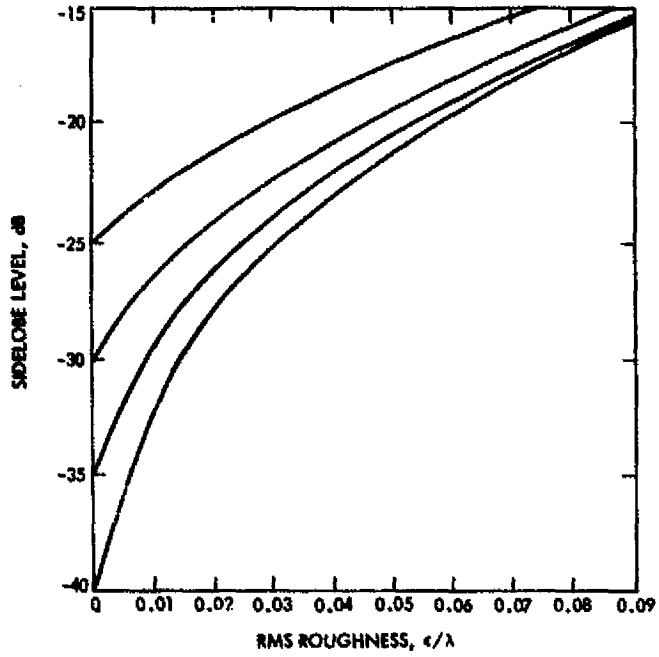

Figure 3. Sidelobe Levels for Various Illuminations as a Function of RMS Surface Roughness

include deployable, erectable, and manufacturable designs. Deployable antennas are launched in a folded configuration and deployed in space; erectables are launched as segments that are assembled in space; and manufacturables are launched as raw materials that are manufactured in space.

2.1.1 Single Reflectors

Single reflector antennas, as the name implies, use one reflector to create a large in-phase distribution of energy by reflecting the energy radiated by a small "point" source feed. Within the scope of this report, front- and offset-fed paraboloid and front-fed spherical antennas will be discussed.

2.1.1.1 Symmetrical Front-Fed Paraboloids. A symmetrical front-fed paraboloid is shown in Fig. 4. While well understood and simple to analyze, they suffer from high blockage due to feeds, feed trusses, and transmission lines. The transmission lines also introduce insertion loss, which increases as the antenna diameter (and focal length) increases. For extremely large antennas it may be advantageous to mount the RF amplifiers near the focal point to eliminate this loss. Blockage causes serious degradation to antenna performance. Figure 5 shows the degradation in peak gain plotted as a function of blockage, while in Fig. 6 the sidelobe level degradation is shown as a function of blockage.

Table 1. Antenna Class Weight Comparison

Antenna	Type	Diameter, m (ft)	Weight, kg (lb)	Weight/aperture area, kg/m^2 (lb/ft^2)
Voyager	Rigid reflector	3.66 (12)	40.8 (90)	4.4 (0.9)
SEASAT-A SAR	Deployable array	10.7 x 2.2 (35.1 x 7.2)	103 (227)	4.4 (0.9)
MIT Dion-Ricardi	X-band waveguide lens	0.76 (2.5)	3.18 (7)	6.8 (1.4)
GE DSCS	X-band waveguide lens	1.22 (4)	13.15 (29)	11.7 (2.4)
Hughes DSCS	X-band waveguide lens	1.27 (4.16)	7.26 (16)	5.9 (1.2)
Ford Aerospace I-5	Rigid reflector	2.44 (8)	9.98 (22)	2.1 (0.44)
Ford Aerospace	TEM lens	1.22 (4)	20.41 (45)	17.4 (3.57)
Lockheed ATS	Unfurlable reflector	9.14 (30)	81.65 (180)	1.22 (0.25)
Hughes SAR	X-band waveguide array	7.32 x 1.07 (24 x 3.5)	159 (350)	20.4 (4.17)

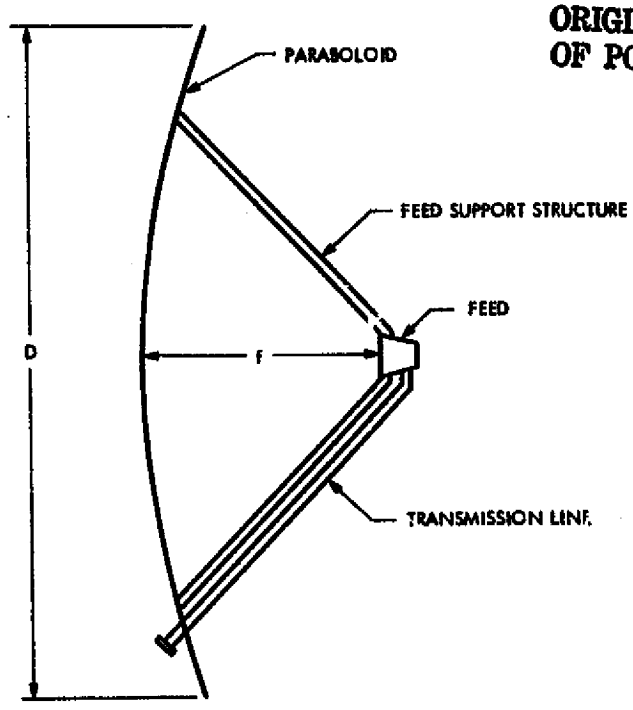

Figure 4. Front-fed Paraboloid

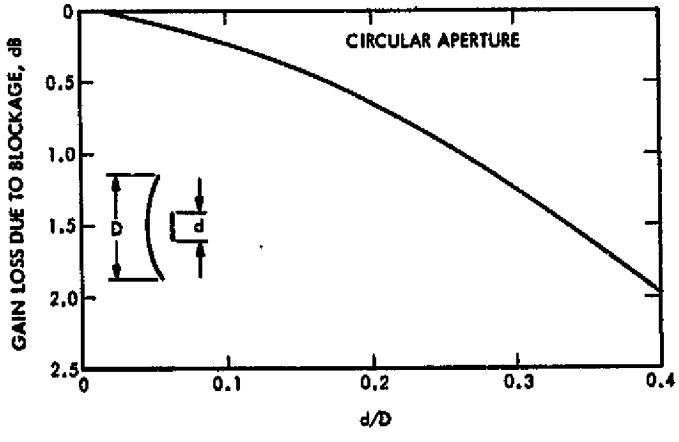

Figure 5. Gain Loss Due to Blockage

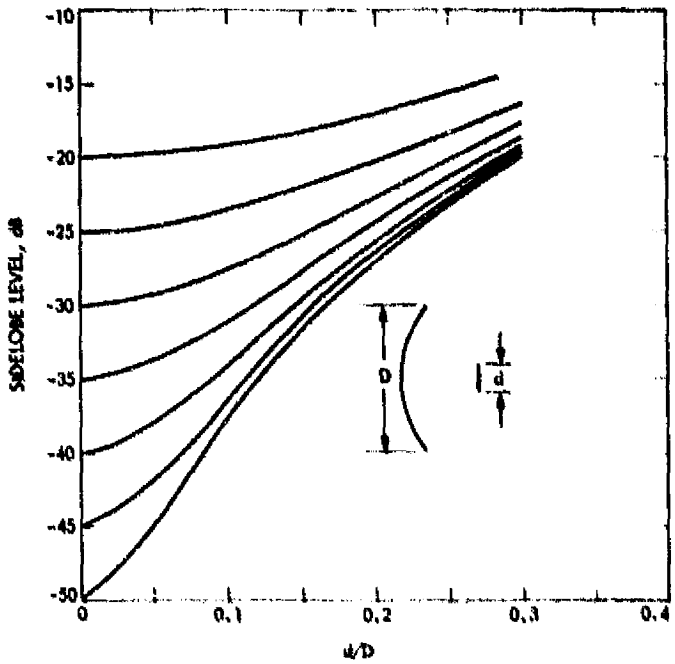

Figure 6. Sidelobe Level vs Aperture Blockage Ratio for a Circular Aperture with Various Illuminations

Off-axis (scanned) beam operation also results in appreciable performance degradation. This degradation is strongly related to the focal length over diameter (f/D) ratio of the reflector and to the aperture illumination function. Figures 7 through 10 (Ref. 28) show beam broadening, loss of gain, and coma lobe degradations as a function of a variable called X, where $X = s\,(D/f)^2/[1 + 0.02\,(D/f)^2]$ (Ref. 28), and aperture illumination function $(1-r^2)^p$. Figure 11 is a plot showing the relationship between X, f/D, and s, the number of beamwidths scanned off axis. Using Figs. 11 and 7 through 10, it can be seen that the performance degradation with beam scan is more pronounced for the small f/D values (0.2 to 0.4) and moderate edge illumination tapers (10 to 12 dB) generally used for front-fed paraboloids than it would be for large f/D and higher illumination tapers.

For instance, using Fig. 11 and picking the curve for a scan of 3 half-power beamwidths off axis, X is about 25 for an 0.3 f/D and about 4 for an 0.8 f/D. Using Fig. 9, the scanned beam gain loss for X = 4 (the 0.8 f/D case) is about 0.1 dB, while it is about 1.5 dB for X = 25 (the 0.3 f/D case), using the 10-dB illumination taper curve for both. Similarly, using Fig. 10, the coma sidelobe is only 18 dB for X = 4 (the 0.8 f/D case), while for X = 25 (the 0.3 f/D case) the coma lobe has degraded to about 9 dB, again using the 10-dB illumination taper curve which gives about a 24-dB sidelobe for an unscanned beam. It can also be seen from Figs. 7 and 8 that the beam broadening with scan is more pronounced for the smaller f/D cases. The effect of the

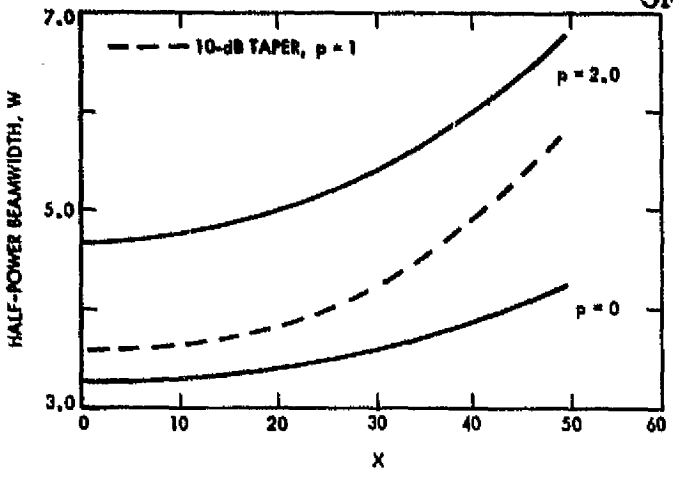

Figure 7. 3-dB Beam Broadening vs X

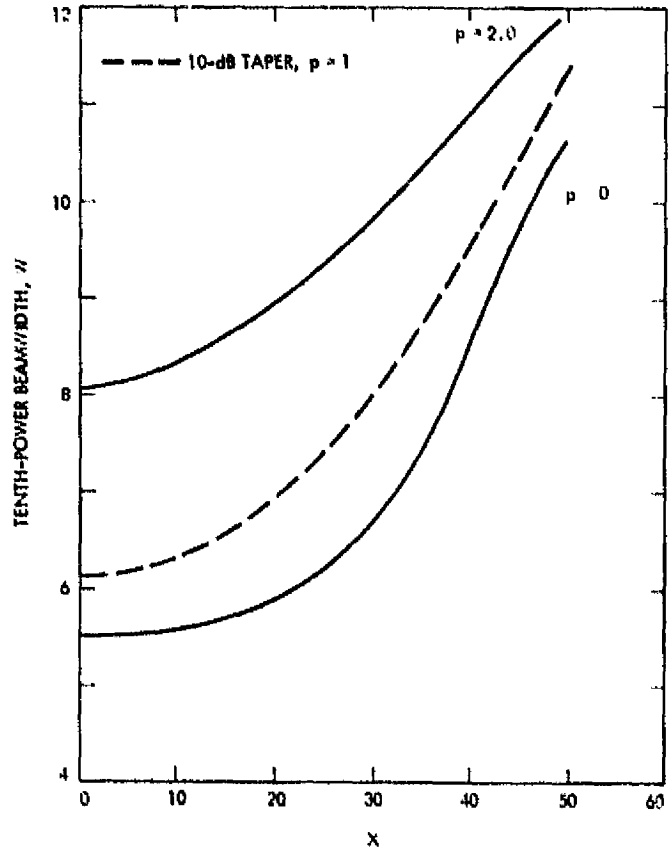

Figure 8. 10-dB Beam Broadening vs X

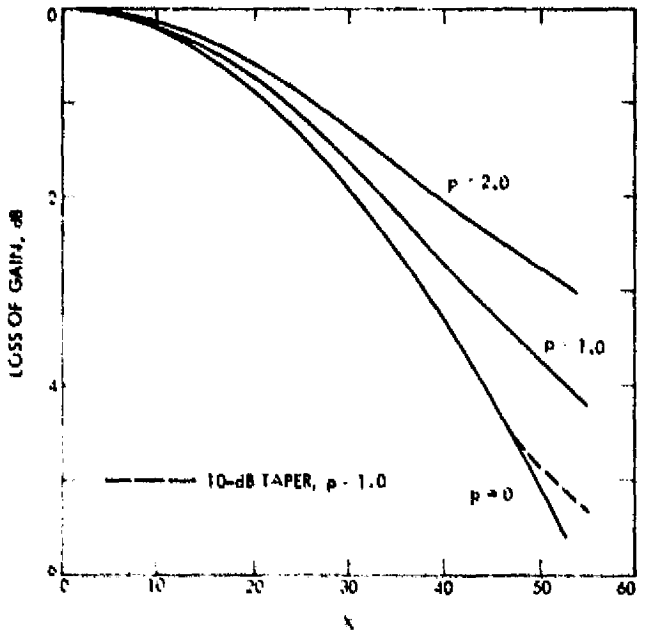

Figure 9. Loss of Gain vs X

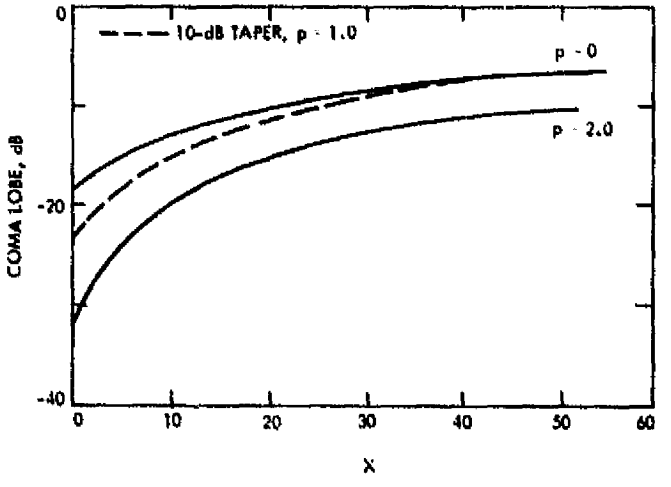

Figure 10. Coma Lobe vs X

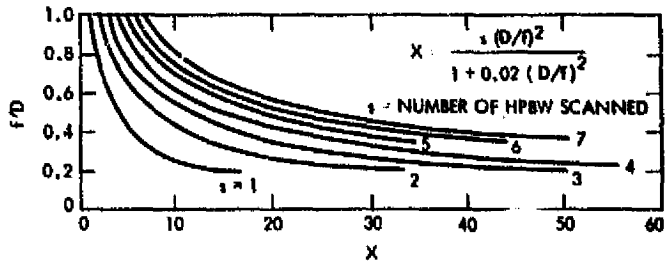

Figure 11. X vs f/D and Scan

aperture illumination function on the scanned characteristics can also be seen from curves 7 through 10. The p = 0 curves correspond to uniform illumination, a theoretical illumination function difficult to approach with a front-fed paraboloid; the 10-dB edge taper curves, for the function $f(r) = 0.3 + 0.7(1-r^2)$, are most similar to the illumination used for many front-fed paraboloids, while the p = 2.0 curves correspond to a very highly tapered illumination function with zero energy at the aperture edge, which improves sidelobe performance at a cost of peak gain. The gain loss with scan as plotted in Fig. 9 is noticeably less for the highly tapered case, though the difference in the change of the other parameters is less dependent on taper.

The curve of Fig. 12 shows the angle to the edge of the reflector as a function of f/D. The larger f/D's have smaller edge angles; to illuminate them with a focal point feed requires a narrower beamwidth feed horn, which forces a larger feed-horn aperture to produce this pattern. Since the path length to the edge of a paraboloid is greater than to the center, space attenuation is added to the pattern of the feed, giving an effective illumination taper greater than the feed pattern taper. As can be seen from Fig. 13, a plot of space attenuation versus feed angle, the larger f/D's (smaller feed angle) give a reduced amount of space loss contribution to taper. This forces an even greater increase in the feed horn size to accomplish the same illumination taper on the reflector. If a more highly tapered illumination is desired for sidelobe reduction, the feed aperture becomes still larger. The larger feedhorn greatly increases the blockage degradation, though this effect becomes less important for a very large reflector, where the feed support strut blockage predominates. Feeds can be loaded to decrease their physical size, though increases in feed mutual coupling cause a reduction in sidelobe performance. Plotted in Fig. 14 (Ref. 28) is beam deviation factor (BDF), defined as beam scan angle over feed offset angle, versus f/D for different illumination functions. It can be seen that BDF increases with f/D for a given illumination function; it also increases with increasing illumination taper for fixed f/D. If the feed offset angle remains constant, an increase in BDF causes an increase in scanned beam angle. Therefore, if f/D remains constant, lowering sidelobe levels by increasing the illumination taper increases both the feed physical size and the BDF. This increases the minimum beam-to-beam separation for a multiple-beam antenna (based on feed physical spacing). If the

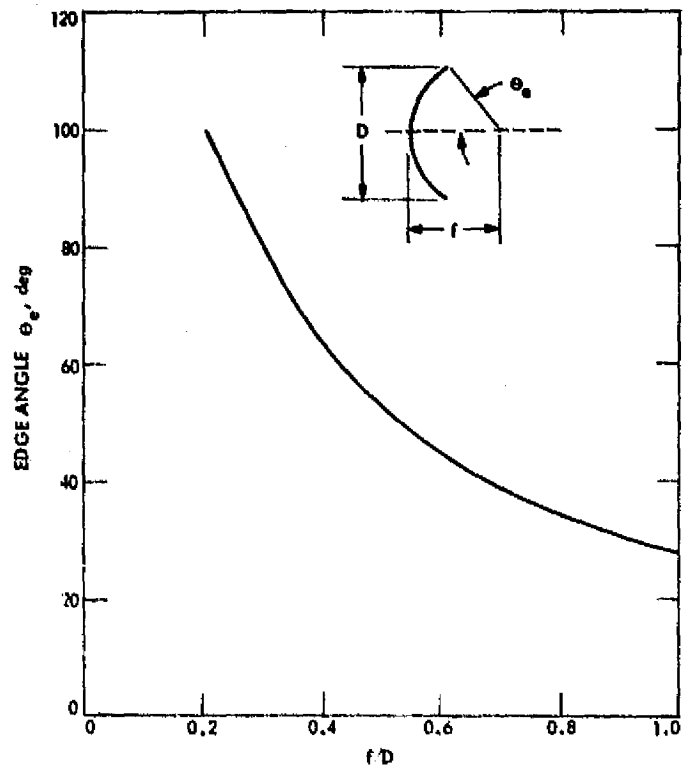

Figure 12. Edge Angle θ_e vs f/D for Paraboloid

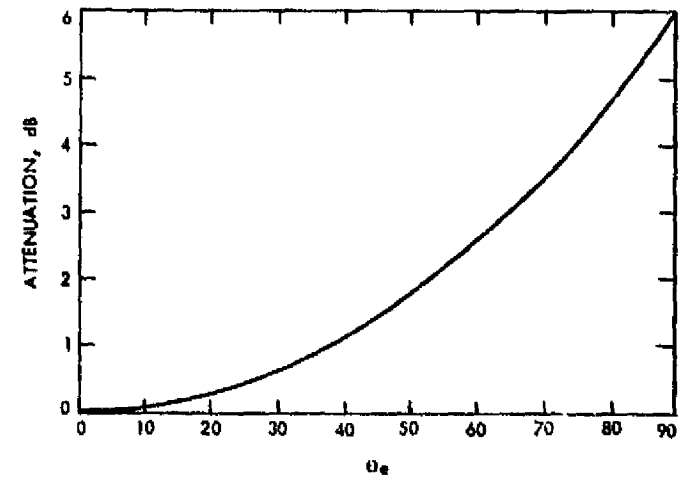

Figure 13. Space Attenuation at Reflector Edge vs Feed Angle

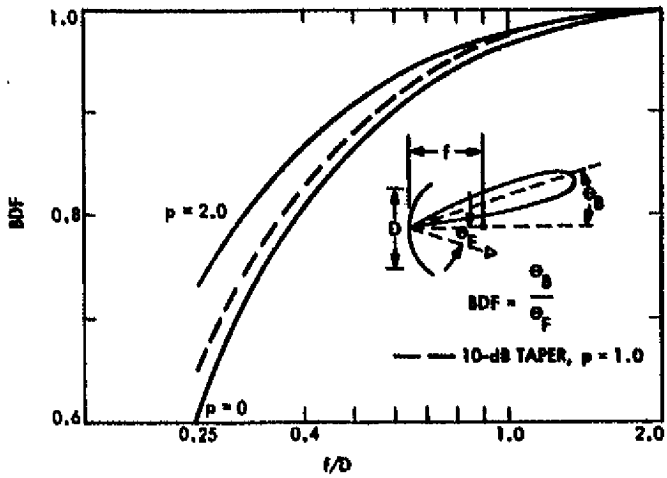

Figure 14. Beam Deviation Factor vs f/D

diameter and the illumination function are fixed, the BDF increase and feed size increase are only partially compensated by the increased focal length effect on the feed offset angle so that the minimum beam spacing increases with f/D increase, as shown in Fig. 15 (Ref. 25).

Figure 16 (Ref. 19) shows peak gain loss versus f/D for a fixed beamwidth, fixed illumination function reflector scanned 5 beamwidths off axis. The blockage loss increases with f/D due to the larger feed required, while the scan loss decreases with increasing f/D. The minimum total loss occurs at an f/D equal to about 1.0. Figure 17 (Ref. 19) shows sidelobe level versus f/D for the same conditions. The coma lobe performance improves with the increasing f/D, while the blockage degradation of sidelobe level increases with f/D due to the larger feed size. The sum of these two contributions also reaches a minimum at an f/D of about 1.0. For this case an f/D of 1.0 seems to be a good choice to optimize scanned performance.

The common front-fed paraboloid with a small f/D is a relatively poor scanning antenna; increasing the f/D to improve scanning increases feed blockage degradation, minimum beam-to-beam separation, and transmission line loss to the feed.

A very large body of design data and experience exists for front-fed paraboloids, as can be seen from the large number of performance curves, most of which came from the literature, included in this section. This makes it one of the most economical types of antenna in terms of design and development time and costs.

The largest unclassified front-fed paraboloid antenna launched to date was built by the Lockheed Missiles and Space Corporation for use on the ATS6 satellite. This 9.1-m (30-ft) diameter 0.48 f/D unfurlable reflector is a front-fed multiple-frequency FBA design with a mesh

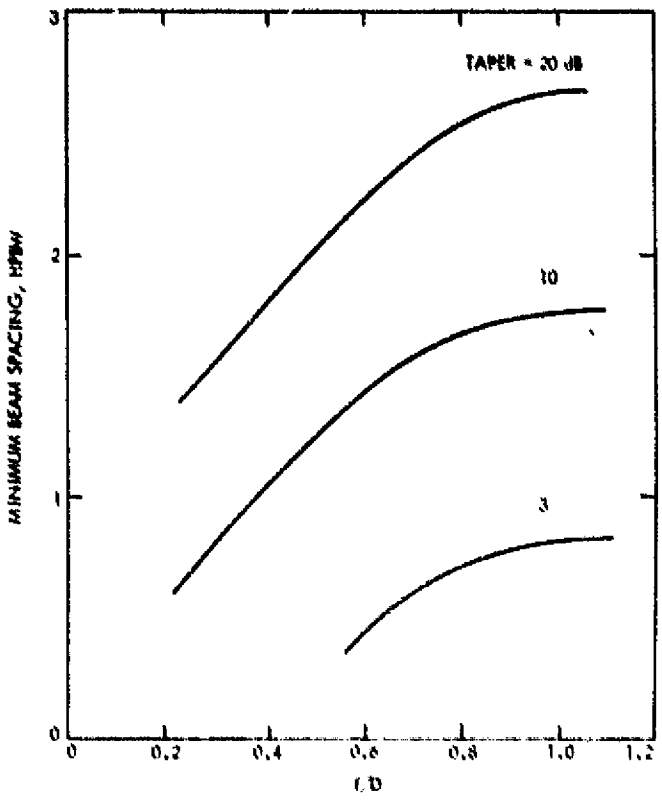

Figure 15. Minimum Beam Spacing vs f/D

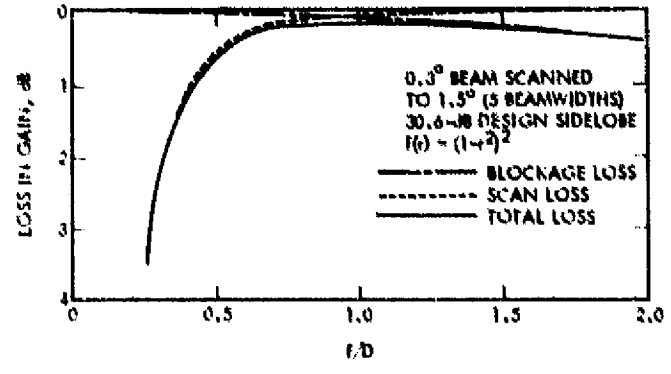

Figure 16. Loss vs f/D at 5 HPBW Scan

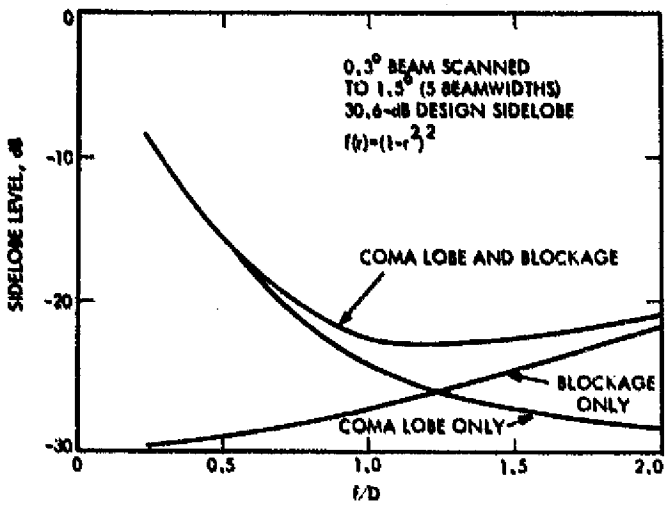

Figure 17. Sidelobe Levels vs f/D at 5 HPBW Scan

surface. The 48 aluminum ribs support a 0.14-cm (0.055-in.) rms mesh surface. The large multiple feeds used for flight operation from VHF through C-band and their support structure contribute large blockage, which significantly degrades flight configuration efficiencies. For instance, S-band overall efficiency is only about 28%. However, during ground testing with only a simple X-band feed and lightweight support structure, it achieved 55% overall efficiency and 0.3 HPBW at 8.25 GHz. The reflector alone weighs about 81.7 kg (180 lb) and stows within a 1.98-m (78-in.) diameter by 20.3-cm (8-in.) high cylinder. A 15.2-m (50-ft) diameter developmental model using graphite epoxy ribs is now being built. Future development of front-fed paraboloids will probably be in the area of increased surface accuracy for higher frequency operation and electrically smaller feed support structures to minimize blockage degradation.

2.1.1.2 Offset-Fed Paraboloid Segments. An offset-fed paraboloid segment, whose elliptical outline projects a circular cross section onto the aperture plane, is shown in Fig 18. D' is the diameter of the original paraboloid which defines the shape of the reflector; the solid line shows a section through the reflector whose diameter is D, while the dashed line shows the section through the unused portion of the paraboloid. The focal length f and focal point are defined by the original paraboloid. The feeds, transmission lines, and support structure are offset out of the aperture and contribute no blockage degradation to overall performance, a substantial advantage if multiple feeds are to be employed. The angle θ_e to the reflector edge can be used with the curve of edge angle versus f/D in Fig. 12 to define an effective f/D for the offset reflector. This f/D can then be used in the curves of Figs. 10 and 11 to approximate the sidelobe scan degradation of the offset reflector. The offset reflector has an effective f/D about twice that of the original paraboloid, which means that the scanned sidelobe performance should be significantly better. The peak gain degradation with scan can

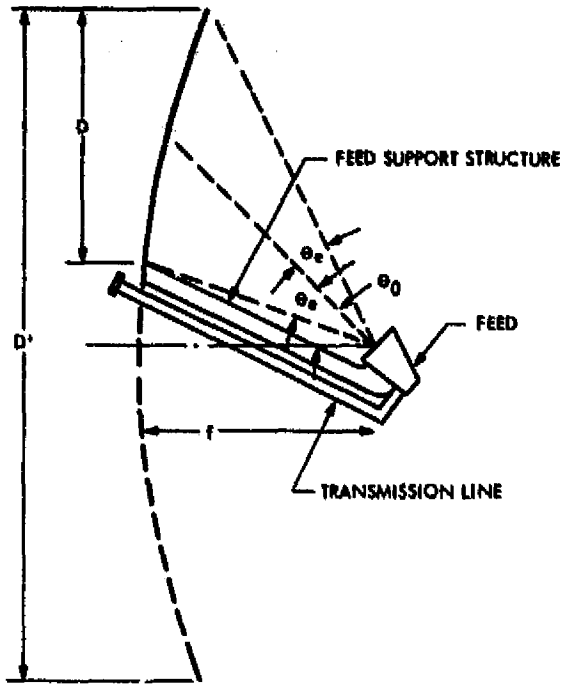

Figure 18. Offset-fed Paraboloid Segment

be predicted (Ref. 24) using the f/D' of the complete parent paraboloid (which was used to define the surface of the offset segment) in the curves of Figs. 9 and 11.

The offset reflector will generate no cross-polarized component if the feed is circularly polarized over the entire included angle. However, the circularly polarized beams will be slightly squinted off the boresite in the plane of symmetry. Figure 19 (Ref. 5) shows that the farther the paraboloid segment is offset, the worse the beam squint becomes for a fixed θ_e (fixed f/D). It also shows that for a fixed angular offset the beam squint increases with increasing edge angle (decreasing f/D). Figure 20 (Ref. 5) shows the measured beam separation between the left-and right-hand beams of an offset paraboloid segment with a 30.5-cm (12-in.) diameter aperture and $\theta_0 = \theta_e = 45^\circ$, illuminated with a 10-dB edge taper at 18.5 GHz. This beam squint causes a slight pointing loss if simultaneous dual polarization is used. The beam deviation factor and scan degradation for the offset paraboloid reflector is not uniform in the various possible scan planes because of nonsymmetry (Ref. 17).

Though the offset reflector antenna, like the front fed, is a poor scanning antenna with a minimum beam spacing very similar to that shown for the front fed, the lack of blockage degradation gives greater freedom to use larger f/D's to achieve a scanning antenna with better overall performance.

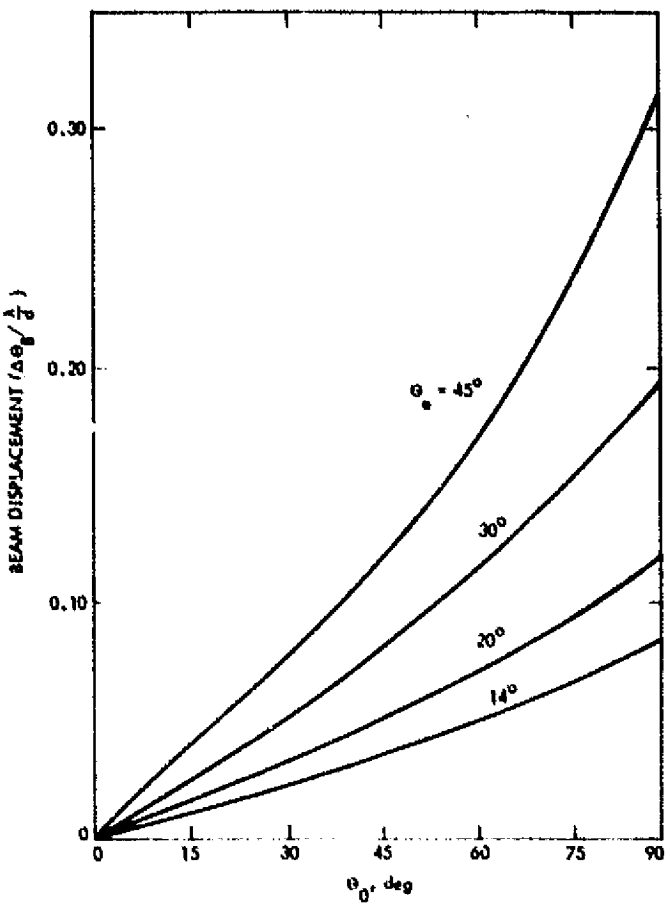

Figure 19. Beam Displacement of Circularly Polarized Excitation for Offset-Fed Paraboloid

Since less design data and experience exists for offset-fed paraboloids, the design and development times and costs will be higher than those for the front fed.

An offset reflector for SUMBA operation with a 2.7-m (9-ft) diameter aperture operating at C-band has been breadboarded at the Ford Aerospace Corporation. It is fed with 78 one-wavelength square dual circularly polarized waveguide feeds (Ref. 15) and a beam forming network. Scans of ±6 beamwidths with about 2-dB gain degradation and a 20-dB first sidelobe have been measured.

The same manufacturer has built 2.4-m (8-ft) flight offset reflectors weighing 9.98 kg (22 lb) each for the I-5 Satellite, using advanced composite materials technology to achieve 0.05-mm (0.002-in.) RMS surface roughness with a thermal coefficient of expansion of 0.18 x 10^{-6} cm/cm/°C (0.1 x 10^{-6} in./in./°F).

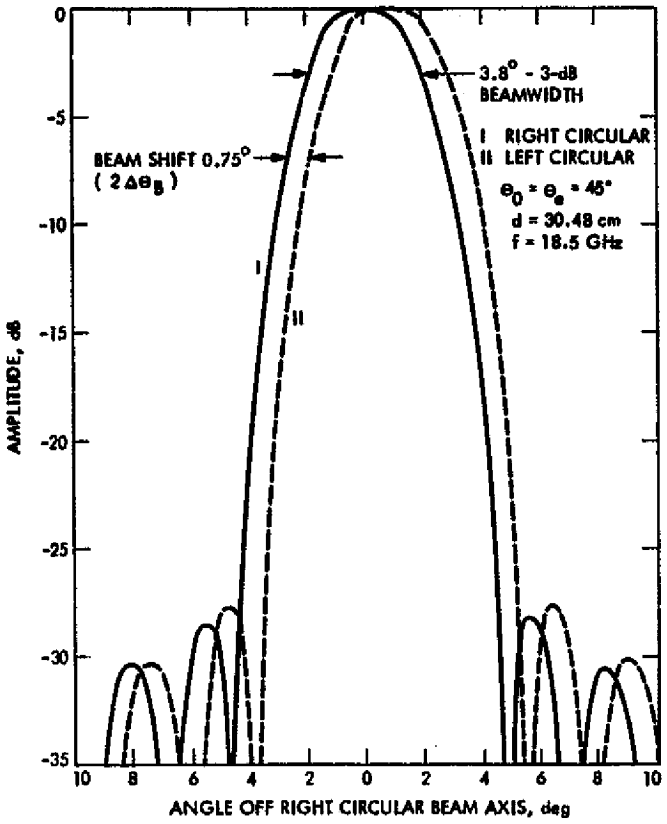

Figure 20. Measured Radiation Patterns of Offset-fed Paraboloid Antenna

A 2.7-m (9-ft) diameter offset paraboloid with an effective f/D of about 1.0 operating at 4 GHz was breadboarded at Lockheed Missiles and Space Company. When fed with a 30-horn feed, 2° beamwidths were achieved with 23 dB on axis sidelobes. To achieve a desired 1.3 beamwidth minimum beam spacing, loaded feed horns were required to avoid feed physical overlap. Scans of ± 4.5 beamwidths were measured with 1.5-dB gain degradation and 13-dB first sidelobe level. An unfurlable model of this reflector weighing 8.16 kg (18 lb) has been built.

2.1.1.3 Symmetrical Spherical Reflectors. The geometry of the spherical reflector is shown in Fig. 21 (Ref. 20). Spherical reflectors can be used if uniform scanned performance is desired. If minimization of degradation due to spherical aberration is desired, illumination can be by line sources, arrays, or lens corrected sources. If the f/D is constrained to be ≥ 0.5, a simpler point source feed can give acceptable performance (Ref. 25). The curve of Fig. 22 shows the approximate best focal length to use with a point source feed in various aperture sizes to minimize phase errors (Ref. 20). Though design data and experience on spherical reflectors are very limited, it can be said in general that spherical reflectors made up of a large portion of a sphere exhibit

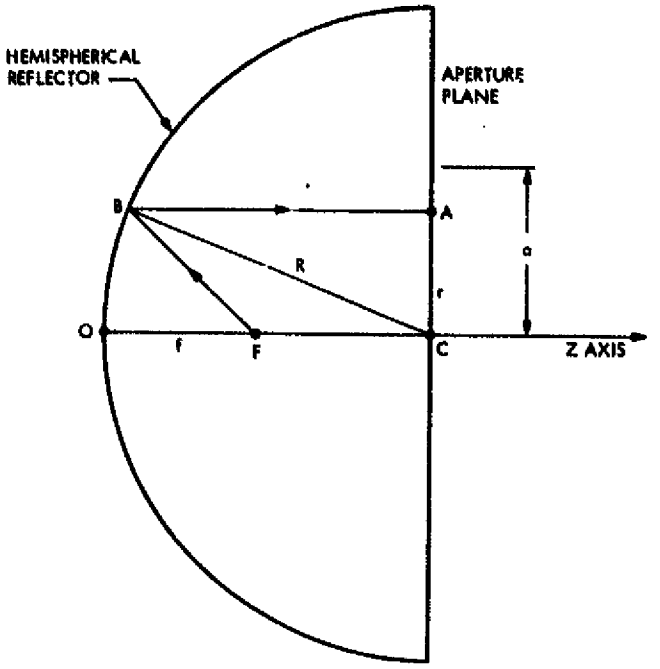

Figure 21. Geometry of a Spherical Reflector

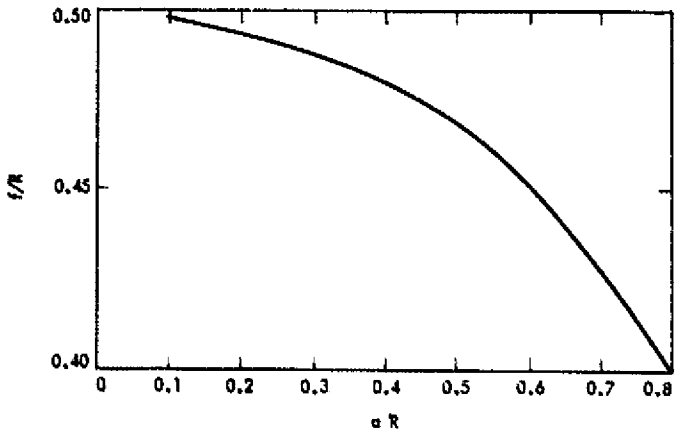

Figure 22. Optimum Focal Length vs Aperture Radius for Spherical Reflector

extremely uniform, though rather poor, pattern behavior over very wide scan angles. Overall efficiency is quite low, due both to spherical aberration and illumination of only a portion of the spherical surface. Use of a reflector made up of a small portion of a sphere yields higher efficiency, good sidelobe performance, and good scan over a smaller scan angle (Ref. 31).

Feed and strut blockage degradation and minimum beam spacing will be similar to that of a paraboloid. Measured scan behavior of a 3-m (10-ft) spherical reflector at 11 GHz with one movable feed is shown in Fig. 23 (Ref. 20). Performance is remarkably uniform out to 70° (approximately 35 beamwidths) of scan, though the on-axis peak gain is only 39.4 dBi. This gain corresponds to an efficiency of less than 10% for the entire 3-m (10-ft) diameter aperture.

Since spherical reflectors are very uncommon and the available design data and experience are extremely sparse, design and development times and costs would be very high.

2.1.2 Multireflectors

Multireflector antennas to be discussed in this section will be limited to those using two reflector surfaces that approximate figures of revolution or portions of figures of revolution. Multireflector antennas can be expected to weigh more than single reflector antennas due to the subreflector, the larger (more directive) feedhorn to properly illuminate the smaller subreflector, and the heavier support structure to support the subreflector. However, the weight (as well as blockage and attenuation) of the transmission line to the focal point is eliminated. Superior electrical properties can be obtained with multireflectors, since the extra reflector gives another degree of design freedom. Though dual reflector antennas would thus be expected to exhibit better scan properties, little data is available.

2.1.2.1 Symmetrical. The best known symmetrical dual reflector is the familiar Cassegrain; less well known is the Gregorian. The geometry of these two designs is shown in Fig. 24. The Cassegrain utilizes the twin focal point properties of the hyperboloid, while the Gregorian uses an ellipsoid subreflector. Spherical main reflectors may also be used with spherical or specially shaped subdishes (Ref. 1). The scan performance of double reflector antennas should be superior to that of single reflector antennas, but they are subject to performance degradation due to subdish and support structure blockage. The feed location is generally near the main reflector vertex, which provides a relatively benign thermal environment. Shaped Cassegrain systems, in which the main and subreflector shapes are slightly altered to achieve the optimum phase and amplitude distribution across the aperture, have been designed and built to optimize on-axis gain. Similar techniques are being developed to improve off-axis scan behavior by altering reflector shapes (Ref. 14).

Most Cassegrain and Gregorian antennas are designed with the feed horn near the main reflector vertex. For these antennas the

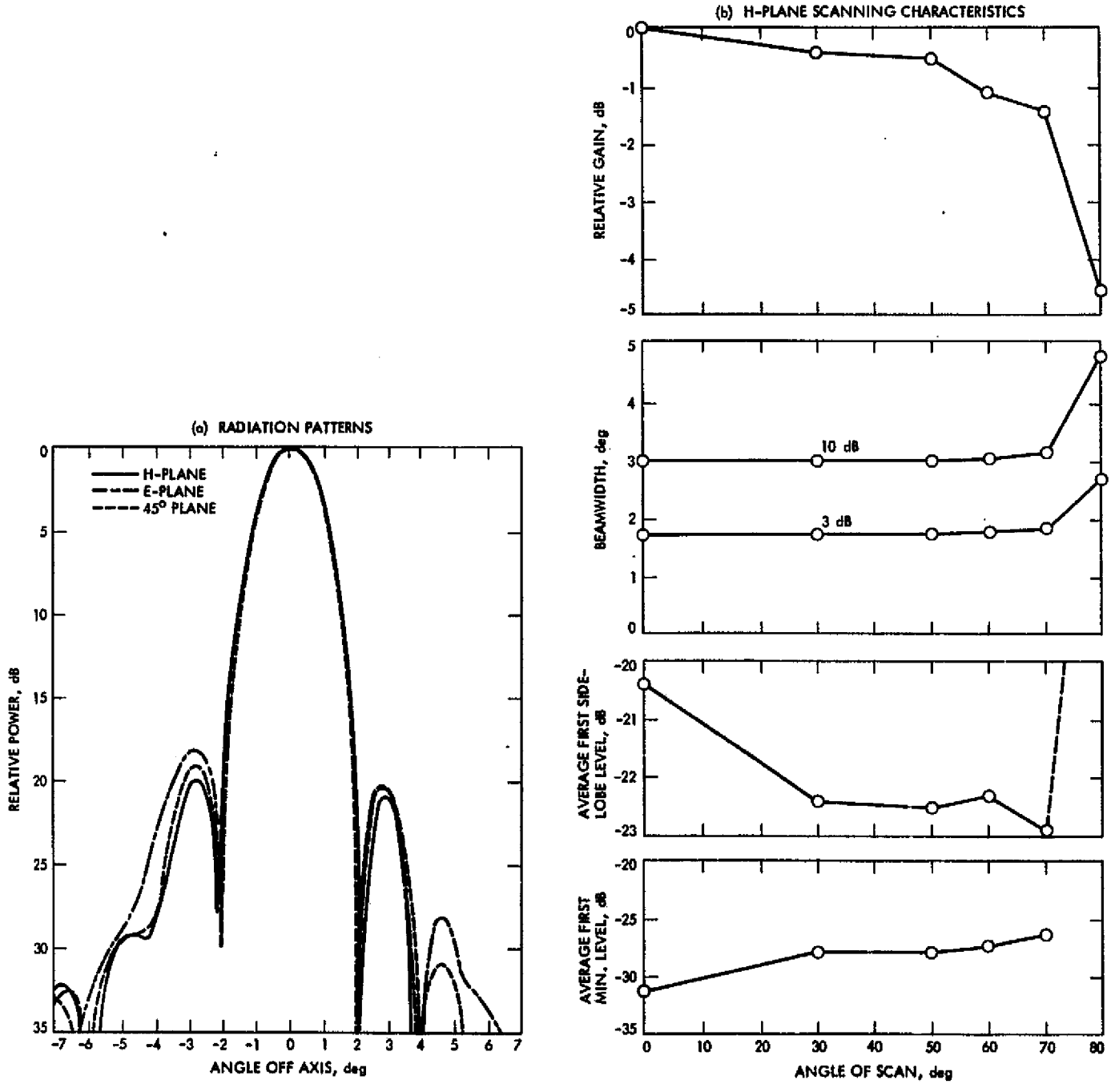

Figure 23. 3-m (10-ft) Spherical Reflector Scan Performance at 11.2 GHz

effective focal length of the system, as defined by the following relationship (Ref. 16), is greater than the main reflector focal length:

$$f_e = \pm \frac{\tan 1/2\ \phi_v}{\tan 1/2\ \phi_r}\ f_m$$

The plus sign is used for Cassegrain systems, the minus for Gregorians; notation is that of Fig. 24. f_e/D can be used in the curves of Figs. 7 through 11 to give an approximation of the scan behavior of simple Gregorians or Cassegrains.

The near-field Cassegrain geometry is shown in Fig. 25. In this configuration a plane wave illuminating the subdish is converted to a spherical wave, which appears to emanate from the focal point of the main reflector. This spherical wave then illuminates the main reflector. An array, lens, or small parabola can be placed so close to the subdish that the subdish is in its near field. This near field is then reproduced, magnified by the ratio of the focal lengths of the two reflectors, in the aperture plane of the main reflector. The secondary beam can be scanned by "tilting" the phase front of the feed. No coma sidelobe degradation occurs since there is no shift of the feed phase center away from the focal point as in other scanned reflector systems.

A large body of design data and experience exists for on-axis simple and shaped Cassegrain systems that will result in low development costs, though off-axis optimized scanners and other dual reflector designs are much less familiar, which will force their development costs into the medium to high range.

A rigid 3.66-m (12-ft) diameter shaped X-band Cassegrain system built by the Ford Aerospace Corporation is in use on the Voyager spacecraft. This FBA, designed for the harsh environment of a Jupiter and Saturn flyby mission, weighs about 51.3 kg (113 lb) and yields about 63% overall efficiency (Ref. 3).

A flight quality 6.1-m (20-ft) diameter dual frequency (1-2 and 3-5 GHz) Cassegrain FBA was built in 1972 by the Lockheed Missiles and Space Company, yielding 30% to 45% overall efficiency with a reflector surface rms designed for 2-GHz operation.

An active reflectarray Cassegrain design conceptualized at the Lockheed Missiles and Space Company is shown in Fig. 26. This concept, based on adaptive feed work described in Section 5.1, is expected to allow SQMBA operation with up to 35 beamwidths of scan.

Another concept being evaluated at the Lockheed Missiles and Space Company involves subreflector shaping to compensate for deployable main reflector periodic shape errors due to mesh deformations between ribs. This concept could result in weight savings for large reflectors by allowing use of a smaller number of ribs than would normally be required to achieve the desired surface rms for a particular frequency.

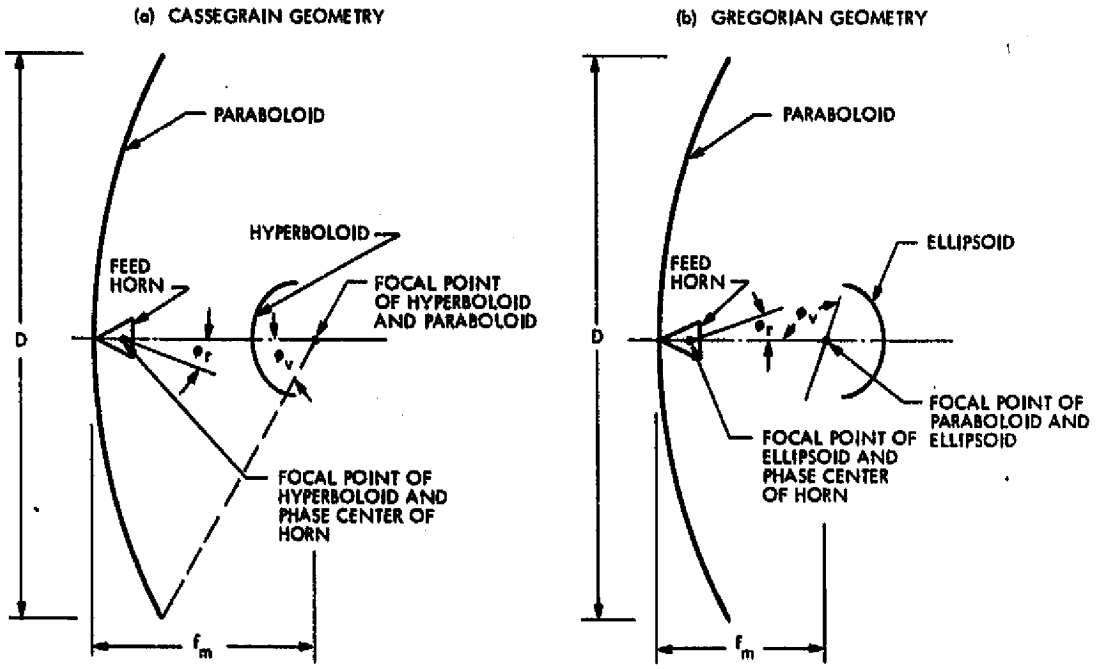

Figure 24. Dual Reflector Geometries

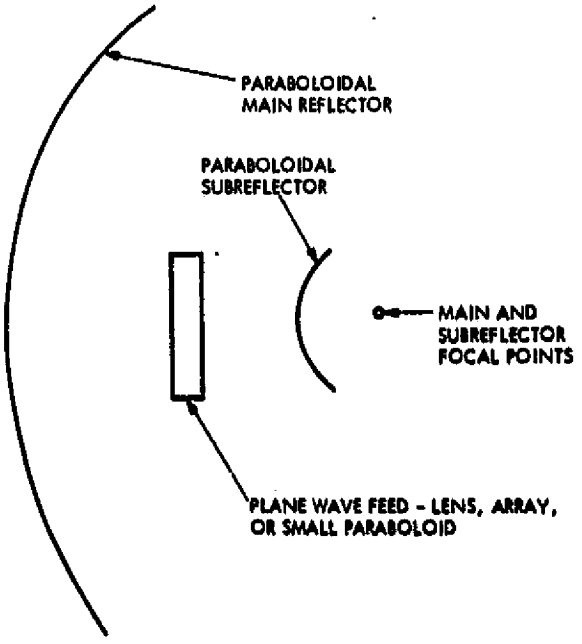

Figure 25. Near-field Cassegrain Geometry

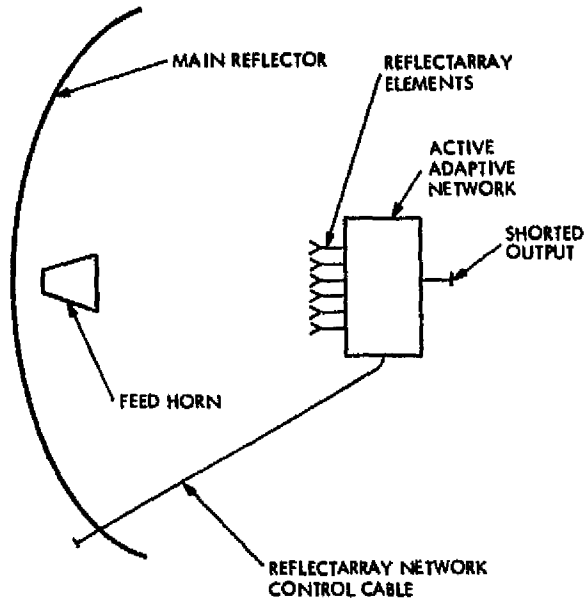

Figure 26. Cassegrain With Reflectarray Replacing Subreflector

A main reflector whose surface is designed to operate at 1 GHz might be usable to 20 GHz through subreflector compensation.

A study performed for ITT Space Communications, Inc., using both spherical and specially shaped subreflectors with a 10.36-m (34-ft) aperture diameter spherical reflector for ground antenna use, predicted overall efficiencies of 45% to 55% (Ref. 1).

A study conducted in 1963 for the Air Force by TRG, Inc., on wide angle properties of dual reflector antennas indicated that, of those configurations studied, the Cassegrain has optimum wide angle properties. Analysis and experiments run on a 1.83-m (6-ft) diameter Cassegrain system at 9000 MHz scanned the beam by moving the feed horn off the main dish axis. At a scan position of 4.2 beamwidths off axis, the measured peak gain was degraded by 1.8 dB, while the worst sidelobe was 9.5 dB down, compared to a worst on-axis sidelobe of 12.7 dB down.

An analytical and experimental study of near-field Cassegrain scanning characteristics was carried out at the Massachusetts Institute of Technology (MIT) Lincoln Laboratory (Ref. 12). A 134-wavelength reflector was scanned 5 beamwidths off axis with a 2-dB loss in peak gain and a 13-dB sidelobe (compared to a 15-dB on-axis sidelobe).

2.1.2.2 Offset. The geometry of an offset Cassegrain system is shown in Fig. 27. This geometry eliminates aperture blockage due to both the subreflector and the feed horns. The f/D is large due to the offset design for the same reason as the front-fed offset, and the effective f/D is even larger due to the Cassegrain configuration. Another config-

uration, shown in Fig. 28, is the "open Cassegrain" (Ref. 6), in which the feed horn blocks the aperture, though the subdish and its support do not. This configuration allows scanning of the beam by rotation around the feed horn axis, which can be an advantage in a ground application since low secondary beam elevation angles can be accomplished with forward (subdish) spillover still directed skyward for lower antenna noise temperatures. Though this is not a strong consideration for spacecraft applications, the "open" configuration would allow a more symmetrical mounting of an offset antenna on a spacecraft.

Figure 29 shows the geometry of a near-field Gregorian antenna in which the subdish is an offset section of a paraboloid which is confocal with the main reflector (also an offset section of a paraboloid). The feed (an array or a lens) is so close to the subdish that the subdish is in its near field, giving essentially plane wave illumination of the subdish. The edge rays in the figure show how the reflector system maps the feed's near-field distribution onto the main reflector aperture. Scanning of the secondary beam is accomplished by scanning the feed to "tilt" the phase front of the illuminating plane wave. The forward spillover is reduced since the feed can be placed very close to the subreflector. Like the symmetric near-field designs, off-axis scanning is free of coma sidelobe degradation.

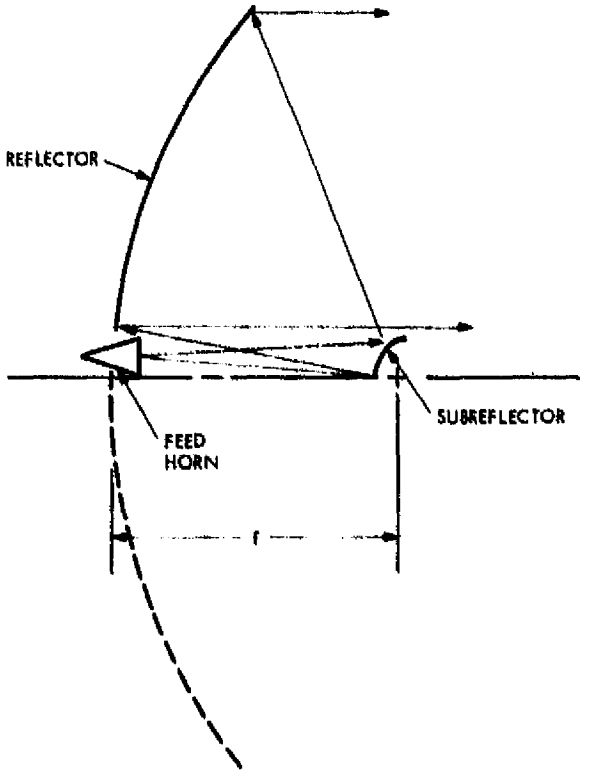

Figure 27. Offset Cassegrain Dual Reflector Antenna

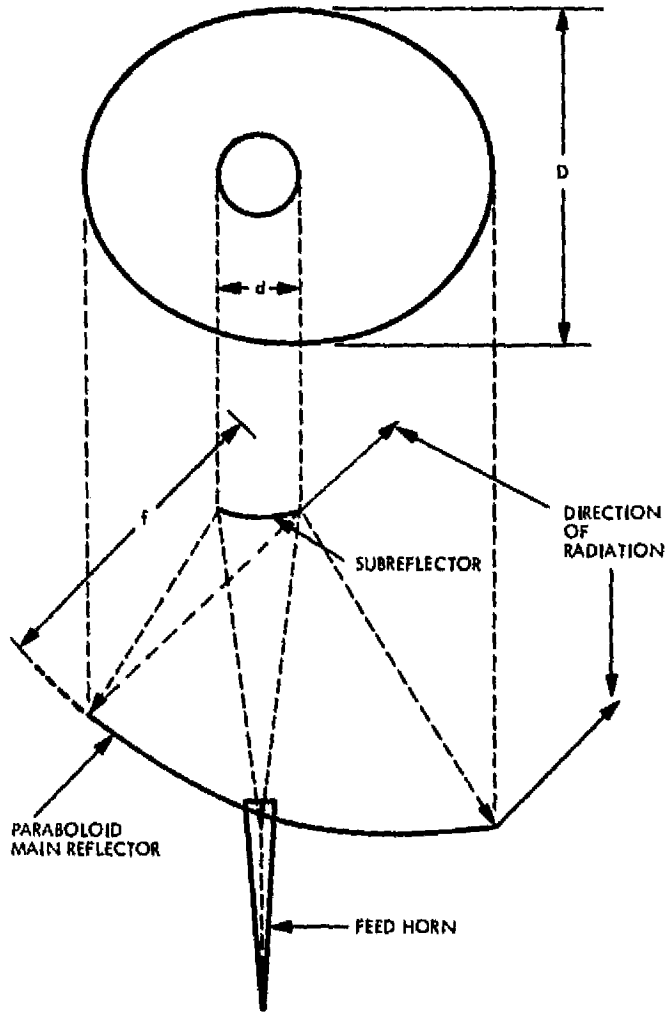

Figure 28. "Open Cassegrain" Geometry

Since offset multireflectors are very uncommon, and the available design data and experience are sparse, design and development times and costs would be high.

A 1.02-m (40-in.) diameter (200 λ) 60-GHz open Cassegrain FBA analyzed and measured at Bell Telephone Laboratories yielded 65% overall efficiency with 24-dB sidelobes.

Another Bell Laboratories study (Ref. 11) analytically compared performance of symmetrical and offset-fed FBA Cassegrain and Gregorian near-field antennas with 13-dB tapers on the main reflector. The results showed that the offsets gave improved on-axis performance; peak gain was 0.7 dB higher, sidelobes were 10 dB lower, and the reflection coefficient was 25 dB better.

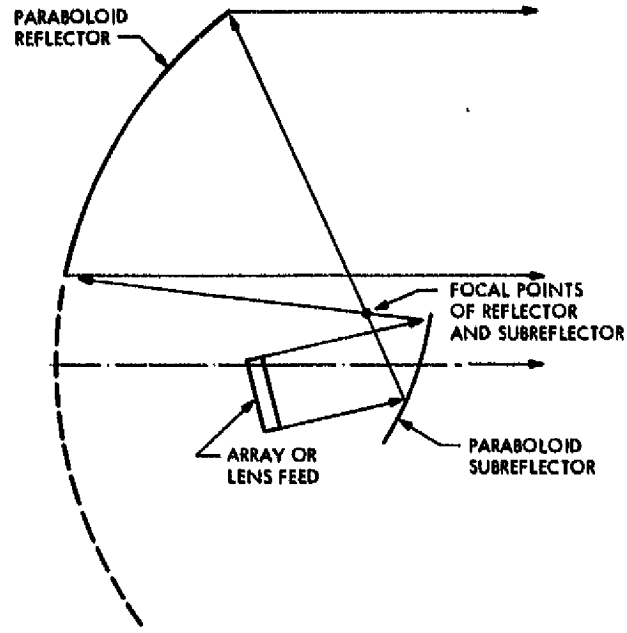

Figure 29. Offset Near-Field Gregorian Antenna

The MIT Lincoln Laboratory analyzed and built a near-field offset Gregorian SQMBA antenna with a 142 λ diameter main reflector and magnification of 4.0 (Ref. 13). Both reflectors are portions of paraboloids. A small focal point fed paraboloid was used to simulate a feed array, with physical rotation used to simulate a feed aperture field phase tilt which scanned the secondary beam. Figure 30 shows measured vertical and horizontal plane scan performance. The vertical plane is the plane of the figure (see Fig. 29) and, as would be expected from an examination of the geometry, yields unsymmetrical scan performance. The parameter θ refers to the feed scan angle, and for small scan angles is linearly related to θ', the secondary beam scan angle, by the magnification. The sidelobe performance with scan is quite good; at 8 beamwidths of scan the sidelobes are still about 20 dB down.

A study by Westinghouse for MIT Lincoln Laboratory developed a computer program to alter the shape of the main and subreflectors of a near-field Gregorian to produce optimum peak gain over a fixed scan range (Ref. 22). The predicted shaped and unshaped performance is shown in Fig. 31. Comparison with the unshaped near-field Gregorian antenna shows that shaping gives 5 dB less peak gain variation with scan accompanied by excellent scanned sidelobe performance at a scan of 8 beamwidths.

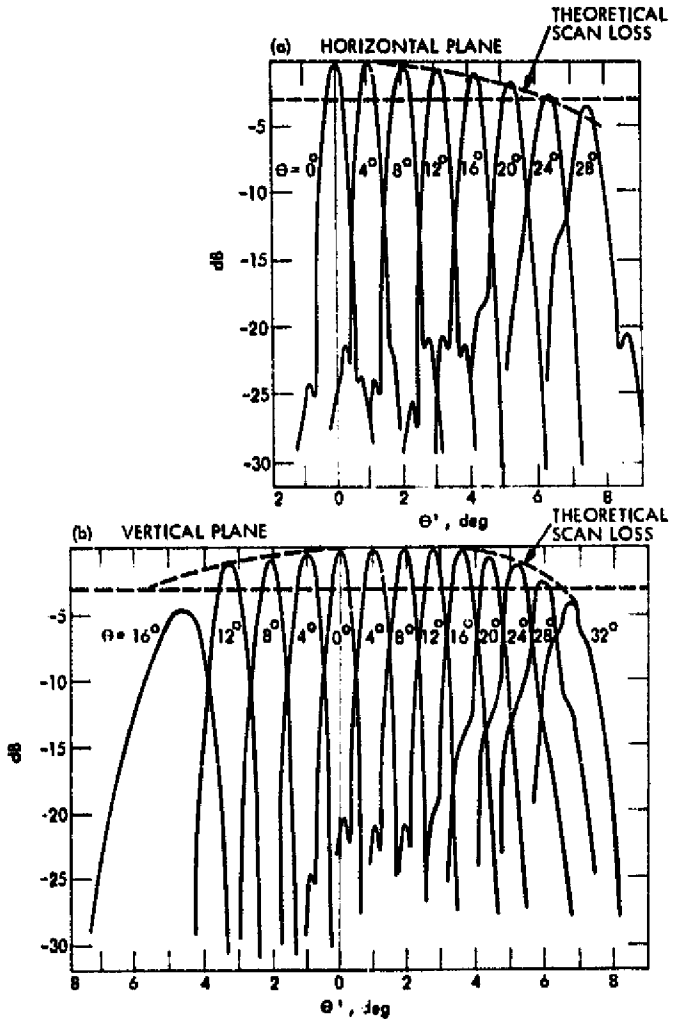

Figure 30. Measured Patterns of Near-Field Offset Gregorian

2.2 LENSES

Of the three classes of antennas discussed, lenses are the least common. Lenses are similar to reflectors in that a small feed can be used to illuminate a large lens. Unlike reflectors, lenses are fed from the rear, eliminating performance degradation due to blockage by feed horns and support struts. In addition, lens designers have three degrees of design freedom: two surfaces and index of refraction.

Lenses, like reflectors, exhibit improved performance with larger f/D. The larger feedhorns then required do not pose a blockage problem as they do with symmetrical reflectors. Lens f/D's of 1.0 or larger are quite common.

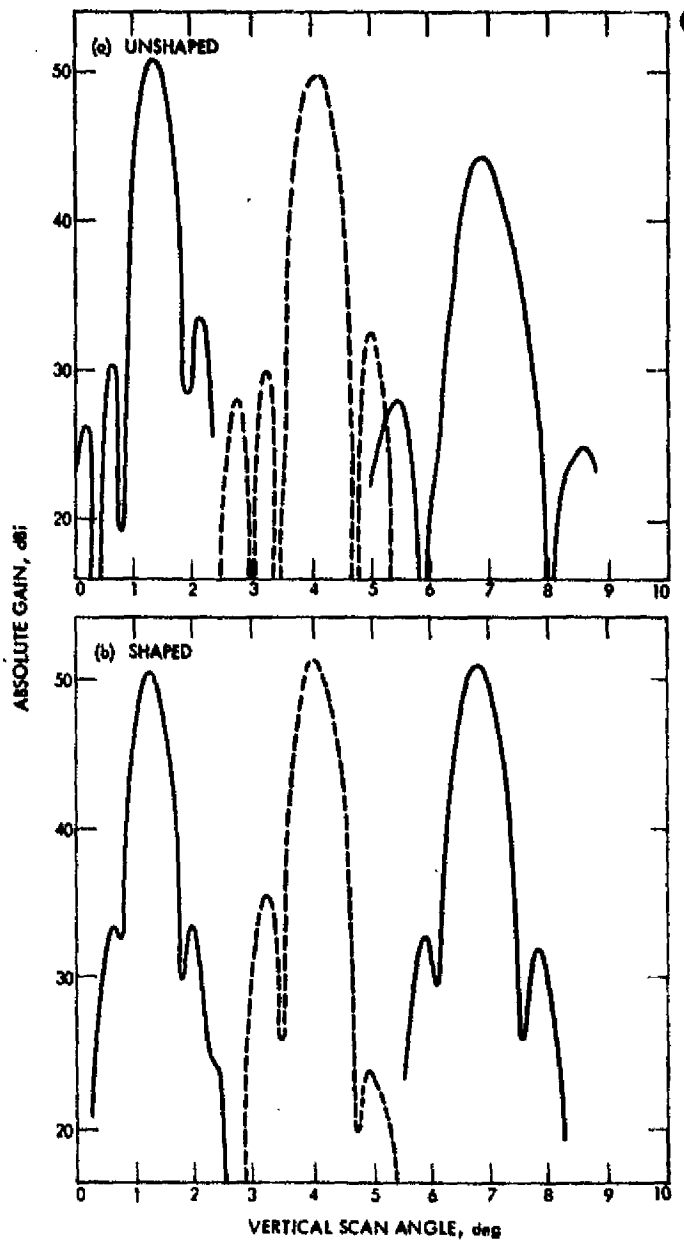

Figure 31. Comparison of Predicted Vertical Plane Scan Performance for Unshaped and Shaped Near-Field Offset Gregorian

The lack of blockage and freedom to use large f/D's has given lenses a reputation as excellent scanners capable of scanning 1-1/2 to 2 times as many beamwidths off axis as front-fed reflectors with the same performance degradation. It should be noted that the improved scan performance is due primarily to the lack of blockage and the large f/D. The actual scan degradation for single surface

lenses can be predicted for various f/D's by the use of Figs. 7 through 11 discussed in the previous section. Figure 15, which shows the minimum beam spacing as a function of illumination taper and f/D, can also be used with lenses. Allowable lens surface contour tolerances are larger than those for parabolic reflectors for the same gain degradation at a given frequency (Ref. 8).

Since lenses are generally fed from the rear, the feeds may be located on the spacecraft structure, providing them with a relatively benign thermal environment. If the outer lens surface is relatively flat, shadowing and thermal distortion problems may be minimized.

The lens presents a moderately difficult design problem because of the small body of design data and experience available. The complexity of lens structures increases the difficulty and cost of their fabrication.

Table 1 shows that lens weights are relatively high.

Very few deployable or space erectable large lens space antenna schemes exist, even in concept form, and none have been demonstrated or flown. While creation and development of practical schemes for very large lens antennas is extremely desirable to take advantage of the RF performance features, it will be expensive and time consuming; due to this it is hard to envision a practical operating very large space antenna of the lens type within the next 10 years.

Two lens types, waveguide and TEM, will be discussed in greater detail. Solid dielectric lenses are extremely heavy and undeployable. Assembling solid dielectric lenses from precut slabs gives erratic performance due to interface discontinuities, and attempts to develop high performance artificial dielectric materials have not given promising results (Ref. 4). For these reaons solid dielectric lenses will not be discussed.

2.2.1 Waveguide Lenses

A simple waveguide lens geometry is shown in Fig. 32. The lens itself is generally made up of an array of square (like an egg crate) or round waveguides. The design is such that the phase length of the sum of the free space and guided paths for all paths between the feed and aperture plane is constant. The phase path length within the guide is based on the guide wavelength, which changes rapidly with frequency, making the lens performance frequency sensitive. The index of refraction of the lens, η, is less than one, giving a lens which is thickest at the edge. A plot of edge thickness divided by lens diameter for a given index of refraction is shown in Fig. 33 (Ref. 26) as a function of f/D.

This shows that the large f/D lenses are considerably thinner, which is doubly advantageous; it results in a lighter weight lens and also improves bandwidth. Waveguide lenses are narrow band devices, the bandwidths being inversely proportional to the edge thickness (Ref. 30) as is shown in Fig. 34. Figure 35 shows a stepped lens, in which a discontinuity with a 360° phase length is introduced when the thickness

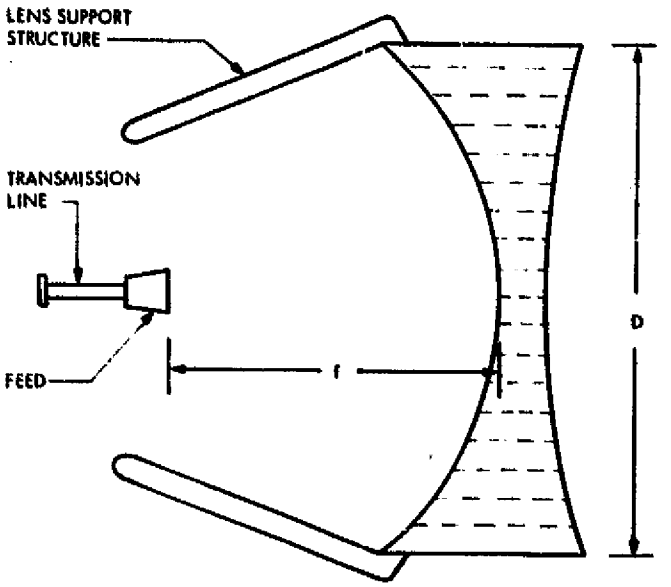

Figure 32. Waveguide Lens

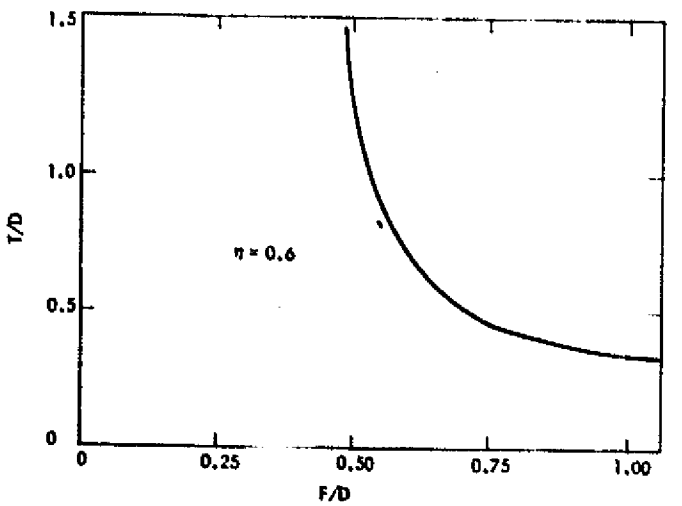

Figure 33. Unstepped Lens Maximum Thickness as a Function of F/D for $\eta = 0.6$

becomes 360° plus t_0. Thus, the maximum thickness will not exceed $(\lambda_0/(1-\eta)) + t_0$. A stepped (also called zoned) waveguide lens yields two advantages over an unstepped one: decreased lens weight and increased bandwidth, though the bandwidth still decreases with increasing diameter. This is seen in Fig. 36, a plot of bandwidth as a function of the number of lens zones. For a 5% bandwidth the diameter is limited to about 30λ. The steps cause peak gain and sidelobe degradation by introducing aperture amplitude distribution errors. Steps on the inside of the lens cause amplitude shadow rings as is shown in Fig. 35, while steps on the outside alter the element pattern (if the lens aperture is considered as an array of square waveguide elements) of the next ring of waveguides, which degrades secondary pattern performance. Some of the bandwidth limiting phase error can be compensated for by moving the feed phase center away from the lens focal point at the limiting frequencies, while leaving it focused at the center frequency by designing a feed whose phase center moves with frequency.

Limited waveguide lens data or experience exists, which will result in medium to high development costs for both on-axis and scanned designs. The complexity of the lens structure will result in medium to high fabrication costs.

The bandwidth limits severely affect the null locations of waveguide lens SUMBA's which employ steerable nulls to reject interfering signal sources. A usable null bandwidth of about 2% is common for a stepped lens of this type. A method has been analytically developed at The Aerospace Corporation to increase the null bandwidth to about 4% (Ref. 7). This method involves using additional steps in the lens to reduce the aperture average phase error. This technique also reduces the overall efficiency and slightly raises the scanned sidelobes of the individual beams when compared with the performance of normally stepped lenses, while increasing the lens weight.

Hughes has built an interesting waveguide lens SUMBA made up of a parallel array of equal length circular waveguide sections, each of which contains a half-wavelength plate. The individual plates are rotated to produce the desired phase shift for that element. Hughes reports a 21° lens edge maximum phase error for this configuration over a 4% bandwidth as compared to about a 35° error for a comparable conventional minimum thickness 3-step waveguide lens. The lens, with a 1.27-m (50-in.) diameter and f/D = 1.52, is fed by 61 X-band horns connected by a corporate power divider summing network with amplitude and phase control to each horn. The feed network introduces about 1.4 dB of loss overall. Operation with a single horn feed gave about 50% efficiency. The extreme feed horn scans to about 4.5 beamwidths off axis with about a 0.3-dB peak gain degradation and 18.5-dB sidelobes (compared to 20-dB sidelobes on axis). For a lightweight spacecraft design, weight would be about 7.26 kg (16 lb) for the lens and 38.56 kg (85 lb) for the feed cluster and beam forming network. A passive phase correcting scheme, which they predict will increase the bandwidth to about 20%, is being developed, though no results are available.

A 0.76-m (30-in.) diameter X-band square waveguide lens was developed at MIT Lincoln Laboratory (Ref. 10) with a predicted bandwidth of about 5%. Measured data indicated that operation over a 10% bandwidth gave a 0.5-dB gain decrease. The 1.0 f/D lens, with a contour chosen to minimize scan degradation, is fed by a cluster of 19 horns.

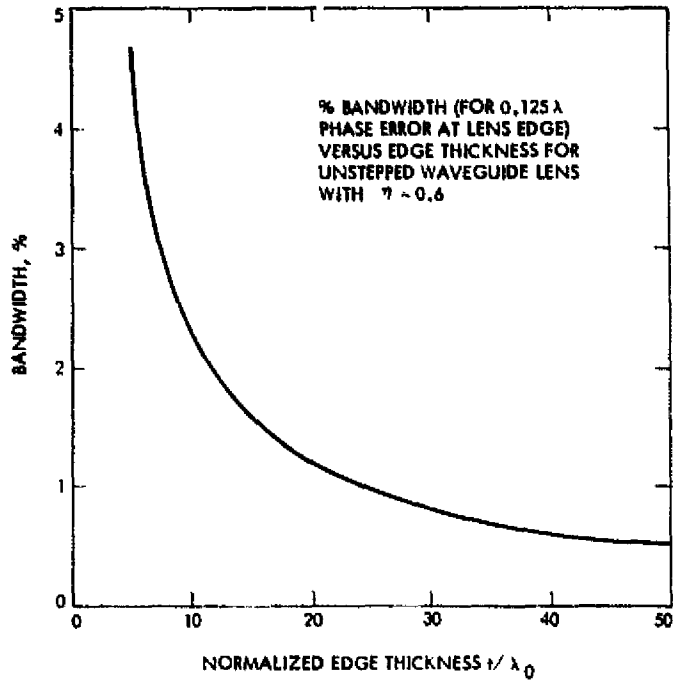

Figure 34. Bandwidth vs Thickness

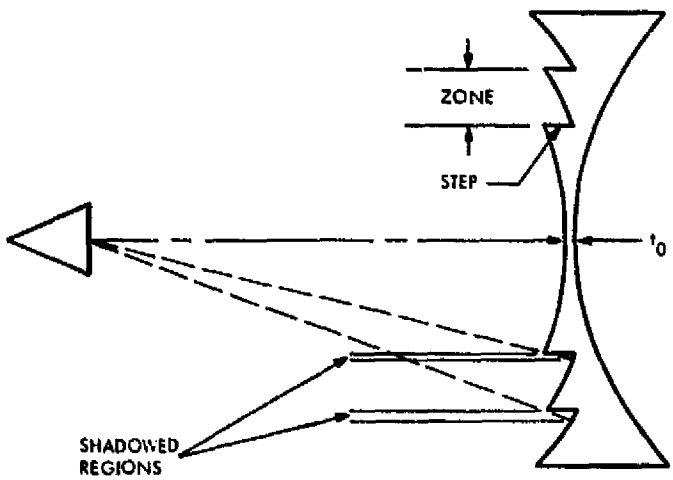

Figure 35. Stepped Waveguide Lens

When scanned about 2-1/3 half-power beamwidths (HPBWs) off axis, the peak gain varies about 0.5 dB and the sidelobes degrade about 3 dB (from an on-axis value of about 24 dB). SUMBA operation is accomplished by feeding the horns with a corporate network using waveguide variable power dividers. Each power divider introduces a loss of about 0.3 dB,

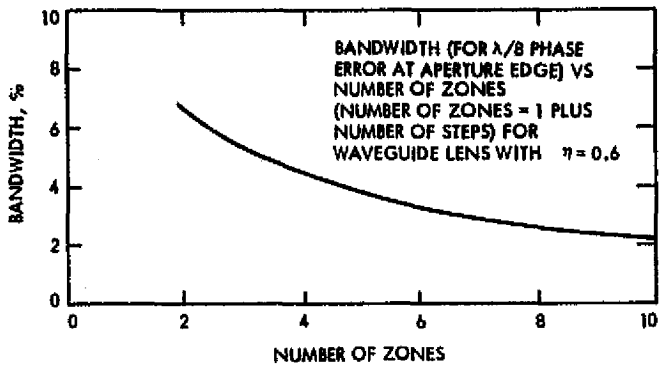

Figure 36. Bandwidth of Simple Waveguide Lens

for a network loss of 1.5 dB. When fed with a single horn feed, the directivity was about 31.5 dB; when all horns were summed through the power divider network, a gain of 20 dB resulted. About 1 dB of gain was lost due to grating lobes of the feed array. A titanium flight model of this lens was built, which weighed 3.18 kg (7 lb).

An X-band stepped lens about 1.22 m (4 ft) in diameter made up of square waveguides was built by Ford Aerospace. When illuminated with a cluster of 61 circularly polarized conical horns with about one wavelength apertures, it created 61 beams with 2° half-power beamwidths and about 5-dB crossovers. The outermost horn created a beam scanned about 9° (4-1/2 half-power beamwidths) off axis. Single feed horn excitation gave about 17.5 dB sidelobes over the field of view with about 0.5 dB gain degradation for the maximum scan position. The overall efficiency was estimated at about 27% for SUMBA operation with a beam forming network.

General Electric has also built a 1.22-m (4-ft) diameter lens with f/D = 1.0 for X-band operation with 61 conical horns, each of which is loaded to increase the aperture illumination taper. With the loaded feeds, about 32 dB of isolation exists between adjacent feed ports. The peak gain scan loss for the maximum scan position is about 0.2 dB. This lens was designed with the Aerospace increased step method to improve the bandwidth. The flight lens weight is about 13.15 kg (29 lb), which would probably be reduced by 50% for a minimum thickness stepped lens. The feed horn cluster weighs about 9.07 kg (20 lb), the beam forming network about 31.75 kg (70 lb), with about 12.25 kg (27 lb) of structure for a total antenna weight of about 66.23 kg (146 lb).

A wideband waveguide lens design has been developed at MIT Lincoln Laboratory (Ref. 9). This compound lens design consists of a conventional waveguide lens and a constant thickness variable phase shift lens. This is probably similar to the Hughes passive phase correcting scheme mentioned earlier. The predicted bandwidth improvement over a minimum thickness stepped lens is dramatic, as shown in Fig. 37. However, this design as described would probably be extremely heavy, though no data on actual models was reported.

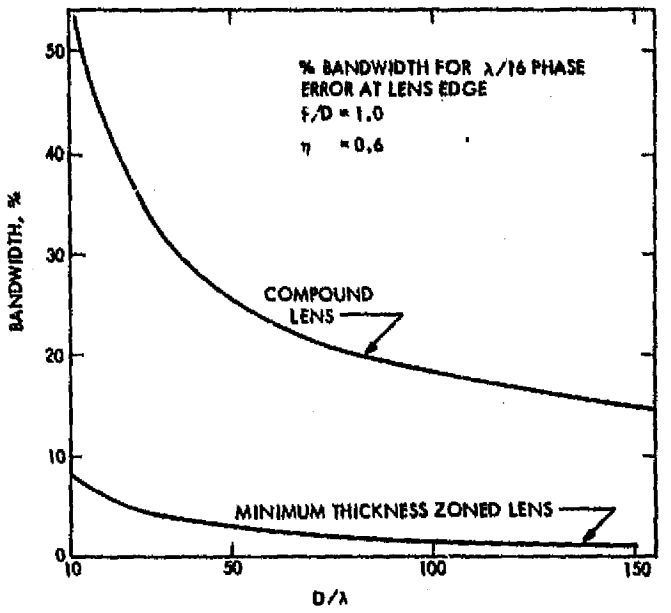

Figure 37. Bandwidth vs Lens Diameter for Compound and Simple Lenses

2.2.2 TEM Lenses

The TEM lens (also called line length or bootlace) concept is shown in Fig. 38. The inner surface of the lens is covered with small elements, which are illuminated by the feed horn at the focal point. The inner elements are connected to the outer elements by coaxial lines operating in the TEM mode. The geometry of the lens and the length of the coaxes control the aperture phase distribution. The outer elements radiate the energy from the coaxial lines to form the final pattern. If the inner surface is spherical, the energy from a feed horn, whose phase center is at the center of the sphere, will reach this surface in phase. Equal length coaxes can then be used to connect to a planar array of radiating elements in order to create an in-phase aperture distribution. This concept gives the designer additional freedom to tailor the aperture distribution to suit his purposes, since the coaxial lengths and interconnections can be chosen for unusual amplitude or phase distributions. With careful design of the radiating elements, high bandwidths--up to an octave--can be obtained. Scan or multibeam capabilities are as good or better than waveguide lenses, but line losses within the lens limit practical operation to below 20 GHz. As with array antennas (see Section 2.3), care must be exercised in the layout of the lens elements to avoid generation of grating lobes.

These lenses are quite complex due to the large number of radiating elements, their many interconnections, and the structure to support them, which also makes them heavy. This also contributes to high design and fabrication costs and lowers the reliability. Very

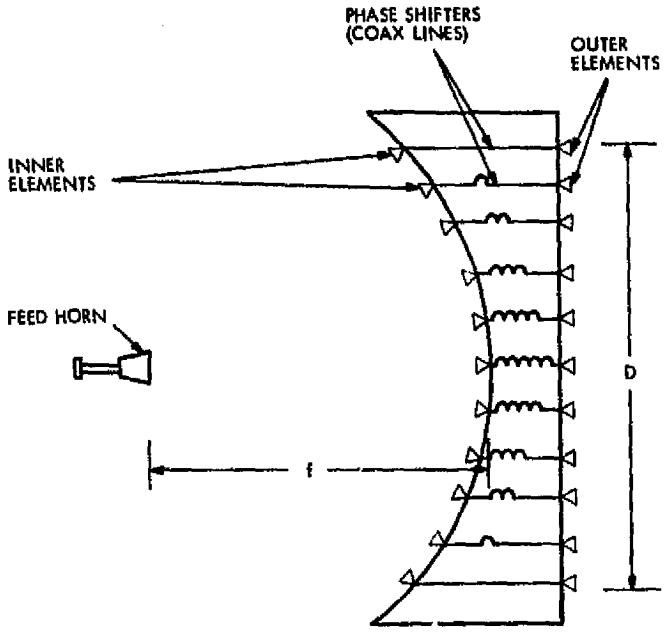

Figure 38. TEM (Bootlace) Lens

limited data or experience exists with these antennas, causing high development costs.

A 1.52-m (60-in.) diameter TEM lens has been breadboarded by the Ford Aerospace Corporation. This lens, designed for operation from 3.7 to 6.4 GHz, uses about 400 printed circuit lens element assemblies, which include orthogonal pairs of inner and outer radiating elements and transmission lines (Ref. 21). The lens is thus designed to radiate whatever polarization the feedhorn produces. The lens f/D is 1.0, and it is illuminated by 85 dual circularly polarized conical horns on about 1λ centers at 6 GHz. A 7-element cluster of feeds per beam is used to illuminate the lens for 6-GHz SIMBA operation and 13 are used at 4 GHz. An extreme scanned (3.2 half-power beamwidths off axis) beam exhibits approximately 0.1-dB peak gain degradation with 32-dB first sidelobes. The weight of a similarly designed 1.22-m (48-in.) diameter flight design is estimated to weigh about 20.41 kg (45 lb) (for the lens alone).

Hughes Aircraft Company is presently doing a feasibility study on an unfurlable 100- to 300-m diameter bootlace lens concept for use from 250 MHz through 2 GHz. The transmission line connecting the two lens surfaces would contain active phase shifters, amplifiers, and control circuitry. Beam shape and scan position would be controlled by adjusting these active components on command from the ground.

Hughes has also built and tested an interesting X-band bootlace lens with a 1.27-m (50-in.) diameter and f/D = 1.52. The lens

itself is made up of 1213 assemblies consisting of helical inner and outer elements connected by coaxial lines and mounted on a spherical surface. The inner and outer helices are counterwound--one is right hand and the other is left hand. The phase adjustment is accomplished by rotation of the elements with respect to each other. This technique allows all elements to be built identically, saving on design and fabrication costs, and is said to give a better bandwidth than a minimum thickness stepped waveguide lens, but restricts the lens polarization flexibility. The lens is illuminated by an array of 61 conical horns with hexagonal apertures, which are fed by a corporate feed network of variable power dividers and waveguide phase shifters. Adjustment (by geared stepper motors) of the network components can be used to shape or scan the beam. The mean total insertion loss of the feed network was 1.35 dB.

2.3 ARRAYS

An array is a periodic collection of radiating elements whose feed points are simultaneously excited with the proper phases and amplitudes to form a desired beam. The arrays considered here will be made up of electrically small elements, such as dipoles, waveguide slots, or stripline patches. When a feed network made up of elements such as coaxial lines, waveguides, or stripline, is used to feed the array, it is said to be a constraint-fed array as opposed to a space-fed array. A horn-fed waveguide lens could be considered a space-fed array. The aperture field of constraint-fed array can be controlled with greater precision than that of other antenna classes, which gives a very good beam shaping capability, especially where greatly different beam shape requirements exist for patterns in different planes. In addition, the use of adjustable phase shifters allows rapid beam scanning. Scanning in one plane can be accomplished by the use of one phase shifter per row of elements; scanning in two planes requires one phase shifter per element. Arrays can be made to yield high efficiencies (90% overall has been claimed for some fixed beam versions) and can also be designed to scan over large angles (up to $\pm 60^{\circ}$) independently of beamwidth and with very predictable scan degradation due to loss of effective area and change in impedance mismatch of the radiating elements. At 60° scan the peak gain can be expected to be about 3 dB below that of the on-axis beam, while the sidelobes degrade about 2 dB. Care must be exercised when choosing the array element spacing to avoid the generation of grating lobes when scanning. If the maximum desired scan angle is θ, the maximum element spacing, d, which avoids grating lobes, is defined by the following relationship:

$$d = \frac{\lambda}{1 + \sin \theta}$$

Elements are normally spaced slightly closer than this limit.

Arrays excel in SOMBA applications, especially where a requirement for large scan angles or various beam shapes at different times exists. However, most constraint-fed arrays pose a very difficult problem if SIMBA operation is required. A corporate-fed array would

require a separate feed network for each beam; if the packaging could be accomplished, the increased complexity and weight would be prohibitive. Control matrices for SIMBA operation have been developed; however, they are as complex, heavy, and costly as the array itself (and often less reliable).

An interesting example of a space-fed array is the reflectarray, shown schematically in Fig. 39. The energy from the feed horn is received by the radiators, passes through the phase shifters, and is reflected from the short, passes through the phase shifters again, and is reradiated by the radiators. The final amplitude distribution is determined by the feed horn and radiator amplitude patterns, and the phase distribution is determined by the phase shifter settings. For SQMBA operation the phase shifter settings can be altered to scan the beam. SIMBA operation could be accomplished by the use of additional feeds, though scan and blockage degradation similar to that of a front-fed symmetrical reflector would occur.

Waveguide arrays, with their usually flat thin structure and good front to back thermal conductivity, are relatively insensitive to thermal deformation, though corporate waveguide feed networks are sensitive. Other arrays, such as the SEASAT-A SAR antenna, a stripline-fed array of stripline patch radiators, have been found to be very sensitive to thermally induced RF performance degradation.

Unfortunately, for large space antenna applications, very few practical deployment schemes exist, and, except for one long narrow array, the SEASAT-A SAR antenna, none have been flown. This restricts the aperture to less than 4.57 m (15 ft) in diameter to fit within current launch shrouds.

Array design is much less predictable than that of other antenna classes due to the technical difficulties in developing corporate feeds, designing for mutual coupling effects, and in predicting total antenna performance based on test results for smaller subassemblies. Arrays are also relatively inflexible; a change in the required aperture distribution often requires a total redesign of the feed network, and sometimes the aperture as well. These characteristics cause arrays to pose a moderately difficult and time consuming design problem, even to experienced array designers. Development costs generally average three times those of a reflector antenna of similar size. Fabrication costs are also high since the number of radiating elements, phase shifters, and other components rises rapidly (proportional to radius squared) as the aperture size is increased, and assembly costs are high due to complexity.

As shown in Table 1, waveguide array weights tend to be high, though the SEASAT-A SAR antenna is quite lightweight. It has been estimated that a 12.2-m (40-ft) diameter unfurlable waveguide array would be 10 times heavier than an equivalent unfurlable reflector.

The recently launched SEASAT-A satellite included a deployable synthetic aperture radar antenna (Ref. 2) built by Ball Aerospace Systems Division with an extension mechanism built by Astro Research Corporation. This FBA is stowed into a 2.2-m x 1.4-m x 0.5-m package, which was

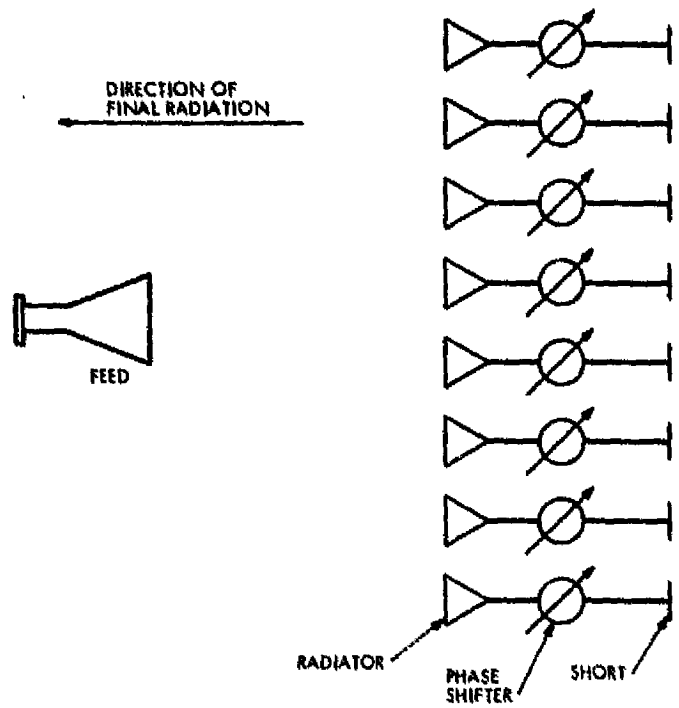

Figure 39. Reflectarray

extended to a 10.7-m by 2.2-m phased array operating at 1275 MHz. The array is made up of stripline patches on a sandwich construction dielectric support with a corporate stripline and coaxial feed network. It yields about 66% efficiency and weighs about 103 kg, including the deployment mechanism.

Hughes has built and space qualified an X-band waveguide FBA synthetic aperture radar array antenna, which is folded once for launch. It deploys to a 7.32-m x 1.02-m (24-ft x 40-in.) aperture, which weighs 158.8 kg (350 lb) including the corporate waveguide feed, support structure, and thermal control blanket. Using rotary joints at the deployment hinge, the overall efficiency is 75%.

Hughes has also built a 4-m by 5-m X-band edge slotted waveguide array for a Meteorological Radar Facility Shuttle experiment. The array receives in a SIMBA mode. Eighty-six 0.5° x 0.81° beams with 4-dB crossovers are formed by detecting the signal phase and amplitude at each row of slots and then digitally combining sets of 3 rows. Though 86 beams are simultaneously formed, the entire aperture is not used for formation of a single beam. The entire field of view is illuminated by a 225-watt average (9 kW peak) transmit signal.

Ford Aerospace and Communications Corporation flew an S-band continuously scanning array on the Synchronous Meteorological Satellite. The array elements were mounted on a right circular cylinder coaxial with

the satellite spin axis. The array was made up of 32 circumferential columns of elements, each column containing 4 elements. Four columns at a time were energized, to produce a 16-element array. When the beam was smoothly steered around the cylinder with variable power dividers, to compensate for the spinning (100 rpm) of the satellite, the peak gain varied about 0.75 dB.

An electronically steerable modular array S-band antenna was developed by Texas Instruments, Inc., for space use. Each array element is fed by a 1.25-watt phase-controlled module. A 48-element array 0.56 m (22 in.) in diameter weighing 11.34 kg (25 lb) scanned to 60° from broadside with 20-dB gain, 10° beamwidth, and 12-dB sidelobes.

A very interesting reflectarray has been developed at Harris Corporation (Ref. 23). It uses the phase shift with physical rotation of a circularly polarized antenna to eliminate the separate phase shifter from the reflectarray elements. The apparent rotation is accomplished by shorting (with diodes) different combinations of the arms of multi-arm spiral radiator array elements. This technique results in lower cost array elements with good performance and lighter weight. A 216-element C-band reflectarray with a beamwidth of about 5° was built and scanned 30° with a peak gain loss of about 1 dB and sidelobes greater than 15 dB down.

A seven-element L- and S-band array about 0.27 m (10.7 in.) in diameter was breadboarded at Texas Instruments, Inc, for shuttle use. Each array module included a 1-watt amplifier, phase shifter, transmit/receive circuitry, and a square spiral radiating element. The array gain was 11.5 dBi on boresite, 5.5 dBi at 60° scan with 40° boresite beamwidth. This array weighed 7.71 kg (17 lb).

SECTION 3

MULTIBEAM ANTENNAS

Much of the recent large space antenna interest has involved multibeam antennas. Many proposed future programs, mostly earth orbiting spacecraft, have included multibeam antennas as part of the spacecraft system, using physical beam separation, different frequencies for different beams, and cross polarized beams to achieve the desired isolation between individual pencil beams. Much of the actual multibeam work done to date has involved multiple feeding of reflectors or lenses to provide many overlapping beams at the same frequency, which can be added for SUMBA operation to yield a broad "flat topped" beam as shown in Fig. 40 (Ref. 10). The individual beam positions are chosen to provide coverage over a geographical or political contour. Discrimination against interfering signals can be provided by switching off one or more feeds to create nulls in the sum pattern in the interference direction. For this application, adjacent beams can cross over at about 4 dB down; however, use of individual beams in the SIMBA mode with this crossover level would result in low isolation levels between beams. Figure 41 shows the approximate isolation due to principal polarization main beam shapes alone. Using this table, it can be seen that beam-to-beam isolation between two adjacent beams is only about 17 dB at the 3-dB down point on either beam for adjacent beam crossovers at the 10-dB level, which indicates that either the entire 3-dB width of the desired beam could not be used, that the beam separations must be kept large, or that frequency or polarization diversity is necessary to maintain higher isolations. In practice actual isolation is a result of much more complex addition of all the lobes of both polarization of all the beams involved.

In an attempt to improve isolation, highly tapered illuminations and large f/D's are used to improve on-axis and scanned sidelobe performance. Typically, a beam-to-beam separation of at least two beamwidths is required for about 30-dB isolation. This two beamwidth separation limitation derives from both beam overlap and feed spacing considerations for simple feeds. However, use of a larger aperture that is more inefficiently (from a peak gain standpoint) illuminated with a cluster of properly amplitude and phase-weighted feeds can create a composite beam with steeper skirts to improve the beam overlap isolation.

Multibeam designs that achieve usable isolations can be expected to yield low overall efficiencies (20% to 30%) due to beam forming circuit losses, aperture inefficiencies, beam coupling, and scan losses. These low efficiencies are often acceptable to system designs.

A SIMBA complex-fed (by a cluster of seven feed horns per beam) TEM lens developed by the Ford Aerospace and Communications Corporation (Ref. 29) operates at both 4 and 6 GHz. At 6 GHz this lens yields ~2.8° 3-dB beamwidth, can be scanned to ±9° off axis with about 0.1-dB gain degradation, and has 32-dB first sidelobes. With six simultaneous noncoherent dual polarized beams no closer that two beamwidths, a 27-dB isolation from <u>all</u> components of the other beams has been calculated.

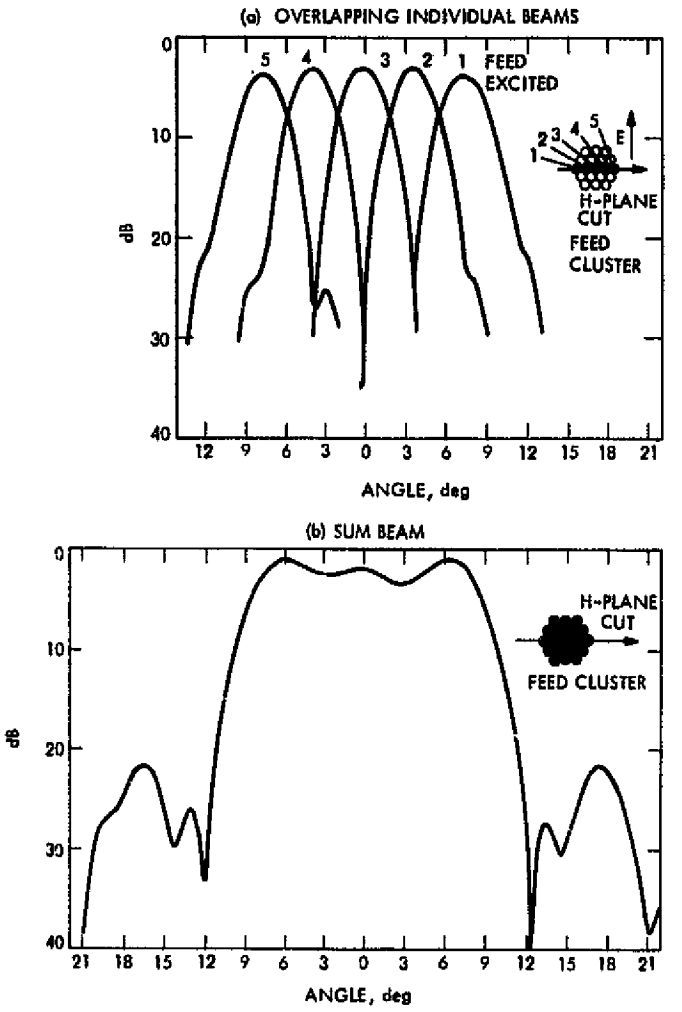

Figure 40. SUMBA Patterns

POSITION DOWN FROM PEAK ON DESIRED MAIN BEAM, dB	CROSSOVER LEVEL OF ADJACENT MAIN BEAMS, dB		
	4	6	10
0	20	25	30
3	2	8	17
6	-4	0	10
10	-9	-6	0
	MAIN BEAM-TO-MAIN BEAM ISOLATION, dB		

MAIN BEAM-TO-MAIN BEAM ISOLATION (dB) BETWEEN ADJACENT BEAMS FOR DIFFERENT BEAM SEPARATIONS AND OPERATING POINTS ON THE DESIRED BEAM.

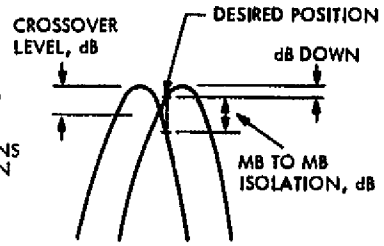

Figure 41. Main Beam Isolation

SECTION 4

APPLICATIONS

From the characteristics presented in Section 2, some general conclusions can be drawn to assist in choosing a specific antenna class as the best choice for certain functional antenna requirements. Each antenna choice will be a compromise between the requirements of high RF performance, low weight, and low cost. It is difficult to draw general conclusions since "good" performance is relative to the criteria for a particular application, and the antenna choice must ultimately be made on a case by case basis. For instance, a minimum scanned sidelobe requirement at four-beamwidth scan may be satisfied at low cost with a reflector antenna by judicious choice of f/D and illumination taper to the detriment of peak gain and weight. This may be acceptable to the spacecraft system even though the general conclusion would have been that reflector scan performance is unacceptable past two or three beamwidths of scan.

For FBA applications requiring modest overall efficiency, in the neighborhood of 50%, the symmetrical front-fed paraboloid provides the advantages of low weight, design complexity, and cost. A higher efficiency requirement, up to about 70%, can be met using shaped Cassegrain designs with a slight increase in weight, design complexity, and cost. Higher efficiency requirements, up to 90%, can be satisfied by phased arrays, though at such a severe cost in weight, design complexity, and cost that consideration should be given to changing to a larger aperture reflector antenna with lower efficiency. An exception to this exists with requirements for nonsymmetric beams greatly differing in various planes, which can often only be satisfied by an array antenna.

SQMBA requirements, especially for large scan angles, are usually best satisfied by array antennas using electronically controlled phase shifters to rapidly change the aperture field. Unfortunately, the weight and cost of such systems become unacceptably high for spacecraft applications as the aperture size becomes large. An attractive solution to this problem is found in the use of a symmetrical or offset near-field Cassegrain or Gregorian reflector system fed by a smaller phased array feed. The reflector system maps the array feed field onto the main reflector aperture, though at a reduced efficiency compared to the array alone. Another method to be considered involves the use of a reflectarray to replace the subreflector of a dual reflector antenna, eliminating the weight and complexity of a corporate feed network at a slight cost in efficiency. Where the number of scanned beams is small or the maximum scan angle is only a few beamwidths, consideration can be given to the use of multiple-fed reflector or lens systems with a probable weight and cost advantage. The antenna designer must compare the specific performance requirements with the abilities of these systems to choose the best design for each particular spacecraft.

SIMBA requirements can usually be met through the use of multiple-fed reflectors or lenses, near-field dual reflectors with multiple-fed lens feeds, or arrays with control matrices, such as the

Butler matrix. The choice will be driven strongly by the maximum scan requirements: single reflectors for scans of 2 or 3 beamwidths, lenses for up to 5 beamwidths, offset near-field dual reflector systems for up to 8 beamwidths, arrays for up to 60°. These general guidelines, however, must be examined with respect to the specific scan requirements involved before the antenna design choice is made. The complexity, weight, and cost will generally increase as the choice moves from single reflectors to lenses or dual reflectors and from that point will increase greatly when arrays are chosen. High beam-to-beam isolation is a common SIMBA performance requirement, which often will force the designer to consider offset reflector systems and complex feed systems for improved sidelobe and beam shape performance.

SUMBA requirements can be met at moderate cost, weight, and complexity by offset multiple-fed single reflectors or with greater cost, weight, and complexity and somewhat better scan performance by multiple-fed lenses. The weight, cost, bandwidth, and detail performance parameters must be traded off to find the best compromise for the specific mission.

SECTION 5

PROMISING CONCEPTS FOR FUTURE DEVELOPMENT

Several concepts that seem to promise advances to the large space antenna state of the art have been encountered. Research and development of these concepts should be considered to define their advantages and limitations for use in realizable spaceborne antenna hardware for future programs.

5.1 ADAPTIVE FEED

Analyses and breadboard measurements have been reported on an adaptive feed system that can be used to greatly improve scan characteristics of a single reflector antenna (Ref. 27). The feed (shown in Fig. 42) consisted of a cluster of radiating elements backed up by phase shifters and a Butler matrix type Fourier transformer. A breadboard model, used to feed a parabolic cylinder, reportedly demonstrated the ability to scan up to 15 beamwidths off axis with a peak gain degradation of only 0.15 dB and first sidelobe degradation of 2 dB. If such a feed can be developed to extend its performance to doubly curved reflectors, it could greatly improve the sidelobe and main beam scan performance of a front-fed or double reflector-fed offset paraboloid segment or lens antenna. The disadvantages of the increased feed cost, complexity, control requirements, and network loss may be acceptable in view of the possible scan performance improvement.

5.2 COMPENSATING SUBREFLECTOR

Unfurlable reflectors require more ribs to operate at higher frequencies (as shown in Fig. 43) in order to avoid excessive performance degradation due to rms reflector contour errors. Reflector weight and cost rise with the number of ribs. A "radially" rippled subreflector has been proposed to compensate for the radial ripples in the main reflector to allow higher frequency use of a "low frequency" reflector for cost and weight savings. An analysis to predict the performance improvement with this scheme is desirable.

5.3 OFFSET SHAPED MULTIREFLECTORS

Offset shaped multireflector antennas appear to promise high performance, lightweight, relatively inexpensive, large space antennas. A study of various configurations and developmental testing of models should be carried out to answer questions such as:

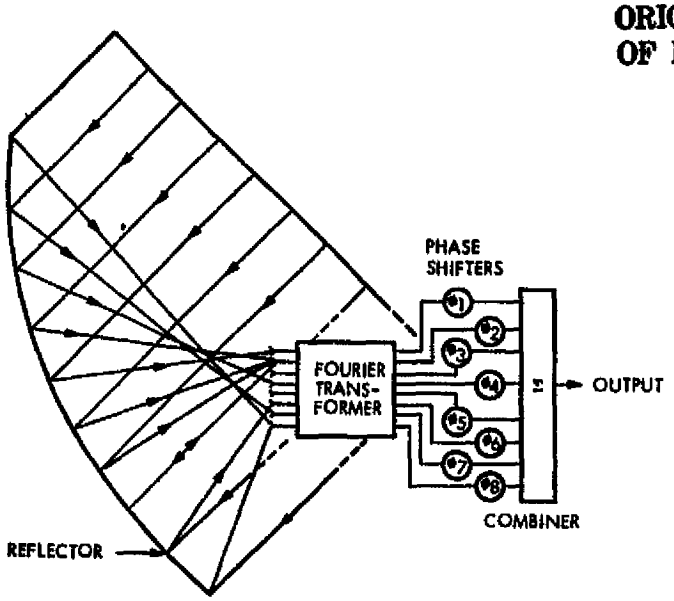

Figure 42. Adaptive primary feed schematic

(1) For a single offset reflector antenna, what is the relationship between f/D, offset angle, illumination function, and beam performance?

(2) For near-field dual offset reflector designs, what is the performance parameter variation with respect to f/D, offset angle, and feed characteristics?

(3) What are the practical advantages and limitations to shaped dual offset reflector designs?

5.4 COMPLEX FEEDS

Much of the performance data quoted here has been for "single" feeds, which implies a single point source radiator. RF sidelobe and beam isolation requirements for scanned or multibeam applications may dictate the use of complex feeds consisting of clusters of radiators fed with varying phases and amplitudes. Studies and developmental tests

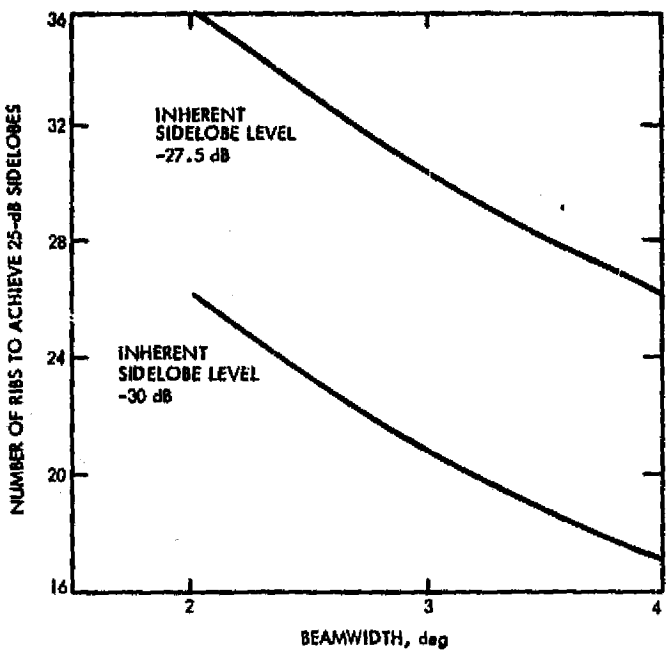

Figure 43. Number of Ribs Required vs Unfurlable Antenna Performance

of these feeds and their controlling networks should be carried out to define their performance characteristics and limitations.

5.5 COMPOUND WAVEGUIDE LENSES

Use of compound lenses for passive phase correcting seems to offer significant bandwidth improvements. Studies and developmental hardware testing should be carried out to define the performance variations and limits with respect to lens f/D, illumination function, and scan especially with a view toward use as near-field dual reflector feeds.

5.6 ANTENNA MEASUREMENT TECHNIQUES

Large apertures pose new RF test problems. Conventional testing on earth for large deployables may be impossible, both because of physical deformations in earth gravity and range size limitations for far-field measurements. In orbit measurement and far-field performance prediction techniques must be developed to verify proper large antenna performance.

5.7 ANTENNA CONCEPT STUDY

A continuing study of activities in the antenna field is desirable to keep abreast of new concepts and industry hardware capabilities for future space applications.

SECTION 6

SUMMARY

Performance estimates for various antenna configurations have been presented. They have been derived based on data gathered during discussions with antenna experts in the antenna industry. JPL sources, and other NASA centers; data presented at the Boston University Communication Satellite Antenna Technology Seminar and at the Technology Service Corporation Phased Array Antenna Seminar; and a study of the literature. In addition, future performance predictions have also been generated, assuming a level of development consistent with the present and no dramatic design breakthroughs. Figure 44 plots the weights of three classes of antennas for aperture diameters from 1 to 100 m. The reflector and furlable TEM lens curves do not include feed or feed support weights, while the furlable waveguide array curve assumes a single fixed-beam corporate feed and a yet to be developed furling technology. Figure 45 plots the costs in 1976 dollars of the same antenna classes for diameters from 10 to 50 m. In Fig. 46 is shown a prediction of developed antenna size out to the year 2000. Table 2 compares existing furling technology with the time necessary to develop the largest practical size for that furling technology. Table 3 compares the general strengths and weaknesses of reflectors, TEM lenses, and waveguide arrays.

Reviewing the characteristics of the three main types of antennas discussed here, the reflector stands out as the most practical choice for many large space antenna applications due to its advanced state of development, light weight (Table 1), high reliability, and low development and fabrication costs. Reflector antenna RF performance, especially for paraboloids, is extremely predictable, a strong advantage for erectable or unfurlable designs; since the feed design is primarily dependent on the f/D ratio and independent of the reflector diameter, feed design can be carried out without a full scale model. Reflectors also (as long as they are operated below the surface rms upper frequency limit) can be reworked or redesigned (in space if necessary) by the installation of different feeds instead of a whole new antenna if user frequency requirements change or if different users require similar diameter antennas operating in different bands, thus reducing development and fabrications costs. For single beam applications, the front-fed paraboloid is the best choice. For multiple beam or scanned beam antennas, the RF degradation due to blockage can be minimized or even eliminated through the use of offset designs, and the poor scan properties of single reflector paraboloids can probably be improved upon to meet or exceed those of lenses by the use of offset shaped near field dual reflectors. If very large scan angles are required, spherical reflectors can be used, at a cost of very low efficiency.

Smaller lenses, arrays, and reflectarrays may be the best choice for the more complex feed systems needed for multiple-beam reflectors. In addition, the lens should be considered for smaller apertures (less than about 4.57 m (15 ft) in diameter to fit within existing shrouds without furling), where good scanning performance is required and the higher weight and cost can be tolerated. The arrays must be

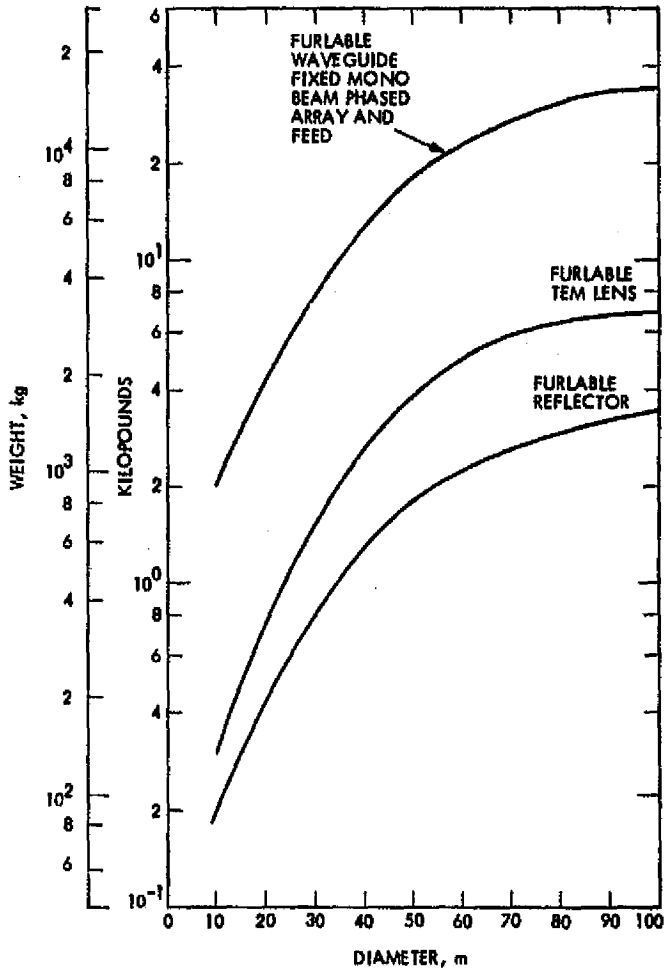

Figure 44. Weight vs Diameter

considered for shaped beams or when single beams must be scanned over very large scan angles, but should also be considered only for apertures less than about 4.57 m (15 ft) in diameter to avoid the complexities of unfurling. These usage suggestions remain only general guidelines; the best antenna compromise for each application must be developed between the system designer and the antenna designer. The spacecraft antenna engineer should be prepared for new and different performance emphasis, especially where scanned or multibeam operation is required.

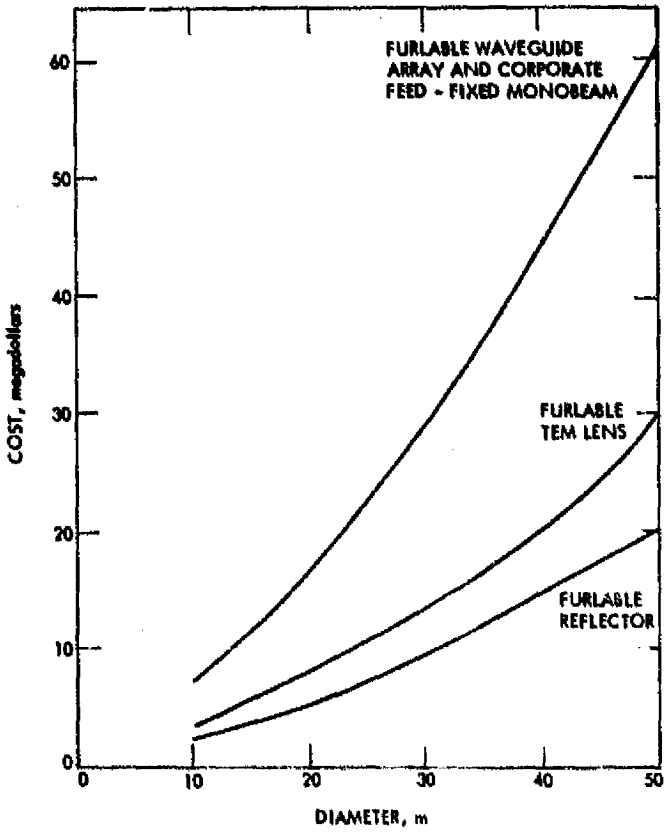

Figure 45. Cost vs Diameter

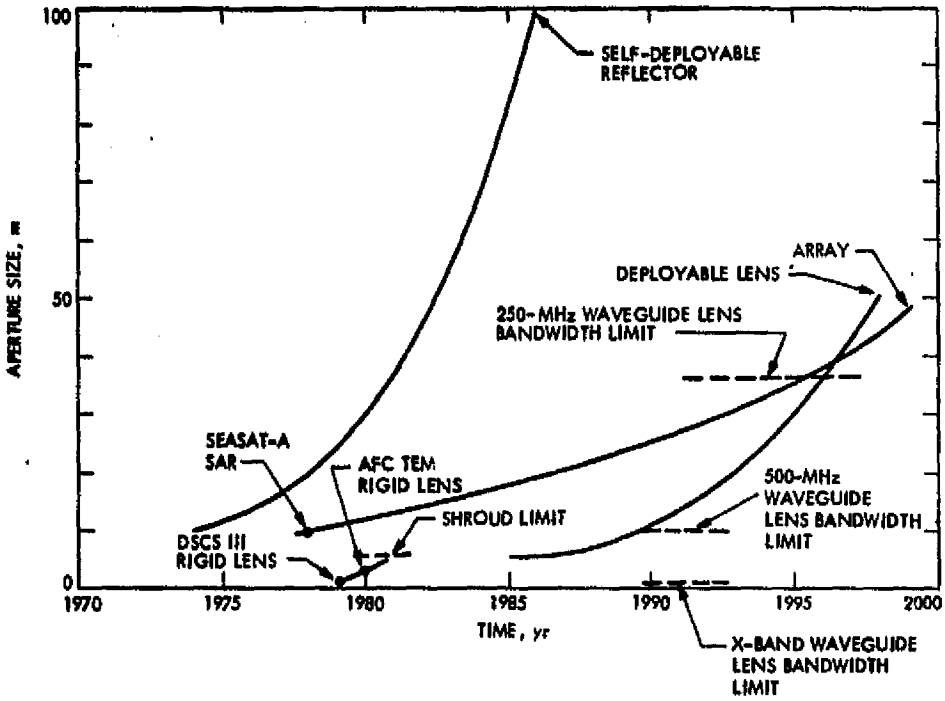

Figure 46. Antenna Size vs Time

Table 2. Furling Technology

Antenna type	Furling type	Development status	Practical size limit	Time to flight development
TEM lens	Maypole	Concept	300-m diam	25 yr
Phased array	SEASAT SAR folding truss	Flight proven 3 x 10 m	20 x 60 m (shuttle pkg)	5 yr
Reflector	Wrapped rib	10 m (ATS6) flight proven	15-m diam	10 yr
Reflector	Maypole	Advanced concept	100- to 300-m diam	20 yr
Reflector	PETA*	Advanced development	125-m diam	10 yr
Reflector	Radial rib	Advanced development	20-m diam (shuttle pkg)	4 yr
Reflector	Sunflower	Advanced development	10-m diam (shuttle pkg)	5 yr
Reflector	Rigidized deployable	Concept	300-m diam	15 yr

*Parabolic expandable truss antenna.

Table 3. Performance Comparison of Different Antenna Classes

Antenna type	Strengths	Weaknesses
Waveguide array	Excellent scanner	Very heavy Very expensive Inflexible design Very difficult deployment Narrowband Poor multibeam ability
TEM lens	Good scanner Thermal stability Broadband Flexible design Very good multibeam ability	Heavy Expensive Complicated deployment Complex
Reflector	Broadband Lightweight Simple Easily deployable Inexpensive Flexible design Moderate multibeam ability	Thermal distortion Poor scanner

REFERENCES

1. Bresler, A. D., "Multiple Beam Spherical Reflector Antenna Systems for Satellite Communications," IEEE Communications Conference, p. 17, 1973.

2. Brejcha, A. G., et al., "The Seasat A Synthetic Aperture Radar Antenna," Synthetic Aperture Radar Technology Conference, Las Cruces, N. M., March 1978.

3. Brejcha, A. G., and Smith, C. A., "Telemetry Antennas for Deep Space Probes," International Telemetry Conference, Los Angeles, Calif., Oct. 1977.

4. Byrnes, P., Multibeam Antenna Study Phase II - Final Report, Document 346314, Lockheed Missiles and Space Company, Inc., June 1973.

5. Chu, Tu-Shing, and Turrin, R. H., "Depolarization Properties of Offset Reflector Antennas," IEEE Trans. Anten. Prop., Vol. AP-20, p. 339, 1973.

6. Cook, J. S., et al., "The Open Cassegrain Antenna," Bell Tel. Syst. Tech. Pub. Monograph 5051, 1965.

7. Coulbourn, C. B., Increased Bandwidth Waveguide Lens Antenna, Report TOR-0076 (6403-01)-3, Aerospace Corporation.

8. Damlamayan, D., "Spacecraft Antenna Research: Antenna Tolerances," in Supporting Research and Advanced Development, Space Programs Sumary 37-66, Vol. III, pp. 43-49, Jet Propulsion Laboratory, Pasadena, Calif., Dec. 31, 1970.

9. Dion, A. R., A Wideband Waveguide Lens, MIT Lincoln Laboratory Technical Note 1977-8, Feb. 2, 1977.

10. Dion, A. R., and Ricardi, L. J., "A Variable Coverage Satellite Antenna System," Proc. IEEE, Vol. 59, p. 252, 1971.

11. Dragone, C., and Hogg, D. C., "The Radiation Pattern and Impedance of Offset Symmetrical Near-Field Cassegrainian and Gregorian Antennas," IEEE Trans. Anten. Prop., Vol. AP-22, p. 472, 1974.

12. Fitzgerald, W. D., Limited Electronic Scanning with a Near-Field Cassegrainian System, MIT Lincoln Laboratory Technical Report 484, Sept. 24, 1971.

13. Fitzgerald, W. D., Limited Electronic Scanning with an Offset-Feed Near-Field Gregorian System, MIT Lincoln Laboratory Technical Report 486, Sept. 24, 1971.

14. Galindo, V., "Brief Tutorial Report on Multiple Beam Reflector Antennas," 1978 (unpublished JPL internal document).

15. Han, C. C., et al., "A General Beam Shaping Technique - Multiple Feed Offset Reflector Antenna System," AIAA, CASI Sixth Commun. Satel. Syst. Conference.

16. Hannan, P., "Microwave Antennas Derived from the Cassegrain Telescope," IRE Trans. Anten. Prop., p. 140, Mar. 1961.

17. Ingerson, P. G., Off Axis Scan Characteristics of Offset Fed Parabolic Reflectors, TRW Systems Group publication.

18. Jansen, J., and Jordan, P. L., Television Broadcast Satellite Study, NASA CR-72510.

19. Kummer, W. H., Final Report for Advanced General Purpose Forces Satellite Antenna Study, TR No. 74-71, SAMSO.

20. Li, T., "A Study of Spherical Reflectors as Wide Angle Scanning Antennas," IRE Trans. Anten. Prop., Vol. AP-7, p. 223, 1959.

21. Mathews, E. W., et al., Advances in Multibeam Satellite Antenna Technology, EASCON, Washington D. C., 1976.

22. Miller, C. J., and Davis, D., LFOV Optimization Study, F19628-70-C-0230, ESD-TR-72-102, MIT Lincoln Laboratory.

23. Phelan, H. R., "Spiraphase - A New Low Cost Lightweight Phased Array," Microwave J., p. 41, Dec. 1976.

24. Rahmat-Samii, Y., "Scattering Characteristics of Large Offset Paraboloids," IOM 3334-78-011, Mar. 23, 1978 (JPL internal document).

25. Rudge, A. W., et al., Study of the Performance and Limitations of Multiple-Beam Antennas, E.R.A. LTD.

26. Rudge, A. W., et al., "Multiple-Beam Antennas: Offset Reflectors with Offset Feeds," IEEE Trans. Anten. Prop., Vol. AP-23, pp. 317-322, May 1975.

27. Rudge, A. W., and Withers, M. J., "A New Technique for Beam-Steering with Fixed Parabolic Reflectors," Proc. IEEE, Vol. 118, pp. 857-863, 1971.

28. Ruze, J., "Lateral Feed Displacement in a Paraboloid," IEEE Trans. Anten. Prop., Vol. AP-13, p. 660, 1965.

29. Scott, W. G., et al., "Design Tradeoffs for Multibeam Antennas in Communications Satellites," International Conference on Communication. Philadelphia, Pa., 1976.

30. Silver, S., Microwave Antenna Theory and Design, p. 408.

31. Woo, R., "A Multiple-Beam Spherical Reflector Antenna," JPL Quarterly Technical Review, Vol. 1, No. 3, pp. 88-96, Jet Propulsion Laboratory, Oct. 1971.

NASA—JPL—Coml., L. A. Calif.